Aspects of Digital Waveguide Networks for Acoustic Modeling Applications

Julius O. Smith III
Center for Computer Research in Music and Acoustics (CCRMA)*
Stanford University, Stanford, CA 94305 USA

Davide Rocchesso
Centro di Sonologia Computazionale
Dipartimento di Elettronica e Informatica
Università degli Studi di Padova
via Gradenigo, 6/A - 35131 Padova, ITALY

December 19, 1997

Abstract

This paper collects together various facts about digital waveguide networks (DWN) used in acoustic modeling, particularly results pertaining to lossless scattering at the junction of N intersecting digital waveguides. Applications discussed include music synthesis based on physical models and delay effects such as artificial reverberation. Connections with Wave Digital Filters (WDF), ladder/lattice digital filters, and other related topics are outlined. General conditions for losslessness and passivity are specified. Computational complexity and dynamic range requirements are addressed. Both physical and algebraic analyses are utilized. The physical interpretation leads to many of the desirable properties of DWNs. Using both physical and algebraic approaches, three new normalized ladder filter structures are derived which have only three multiplications per two-port scattering junction instead of the four required in the well known version. A vector scattering formulation is derived which maximizes generality subject to maintaining desirable properties. Scattering junctions are generalized to allow any waveguide to have a complex wave impedance which is equivalent at the junction to a lumped load impedance, thus providing a convenient bridge between lumped and distributed modeling methods. Junctions involving complex wave impedances yield generalized scattering coefficients which are frequency dependent and therefore implemented in practice using digital filters. Scattering filters are typically isolable to one per junction in a manner analogous to the multiply in a one-multiply lattice-filter section.

*`http://ccrma.stanford.edu/`

Contents

1 Introduction

The theory of lossless scattering of traveling waves has had an enormous influence on theory and practice in science and engineering. For example, classical scattering theory has found applications in transmission-line and microwave engineering [3], geoscience and speech modeling [39, 35], numerically robust filter structures [27, 35, 111, 113, 112, 114, 110], and estimation theory [9]. Moreover, signal processing models of acoustic systems based on a sampled traveling-wave physical description have recently led to extremely efficient structures for musical sound synthesis based on physical models [93, 97, 118, 115, 134, 76, 100] and for delay effects such as artificial reverberation [91, 106, 79, 122, 84, 125].

The solution of the wave equation in terms of traveling waves began with d'Alembert's first publication of it in 1747 [20]. While it may seem likely that scattering theory would have developed with transmission-line analysis in the early part of this century, the concept of the scattering matrix was introduced from general physics to the microwave engineering literature in 1948 (see, e.g., [3, p. 851]). The scattering formalism was developed independently and simultaneously for lumped networks by Belevitch [3, p. 851]. Since then, many fruitful lines of development have grown from the traveling-wave formalism, including results in insertion-loss filter theory, distributed amplifier design, the design of n-ports in telephone applications, wave digital filters, the applications mentioned in the previous paragraph, and the many results discussed in the references.

1.1 Digital Filters as Physical Models

The mainstream literature in digital signal processing does not routinely include methodology for using digital filters as physical modeling elements. On the other hand, literature on general numerical simulation techniques for physical dynamic systems does not generally cover relevant good practice in digital signal processing. Recent applications [91, 56, 64, 122, 134] have shown that many benefits can be derived from taking a physical point of view with respect to digital filtering computations. For example, robust, rapidly time-varying, nearly lossless digital filters (such as needed, e.g., for a guitar string simulation) can be developed more easily using a physical approach, and conditions for the absence of unnatural artifacts become more clear. Moreover, *nonlinear* extensions are much more straightforward when there is a physical interpretation for each of the processing elements. While some benefits of the physical modeling perspective have been realized in the form of general-purpose digital filter structures with good numerical properties, such as ladder and lattice filters,[1] more general use of signal processing elements and analysis/optimization methods in physical modeling applications appears to be rare.

The original Kelly-Lochbaum (KL) speech model [39] employed a ladder filter with delay elements in physically meaningful locations, allowing it to be interpreted as a discrete-time, traveling-wave model of the vocal tract (see the allpass portion of Fig. 5 for a similar diagram). Assuming a reflecting termination at the lips, the KL model can be transformed via elementary manipulations to the ladder/lattice filters used in linear predictive coding (LPC) of speech [92]. The early work of Kelly and Lochbaum appears to have been followed by two main lines of development: (1) "articulatory" speech synthesis which utilizes increasingly sophisticated physical simulations [50, 22], and (2) linear predictive coding of speech [57]. The all-pole synthesis filter used in LPC, when implemented as a ladder filter, can be loosely interpreted as a transformation of the KL model

[1] Following previous usage conventions, we use the term "ladder filter" when the graph of the filter is planar, and "lattice filter" when the graph is non-planar.

[57]. There have been ongoing efforts to develop low bit-rate speech coders based on simplified articulatory models [89, 29]. The main barrier to obtaining practical speech coding methods has been the difficulty of estimating vocal-tract shape given only the speech waveform.

There have been a few developments toward higher quality speech models retaining the simplicity of a source-filter model such as LPC while building on a true physical model interpretation: An extended derivative of the Kelly-Lochbaum (KL) model, adding a nasal tract, neck radiation, and internal damping, has been used to synthesize high-quality female *singing* voice [14]. *Sparse* acoustic tubes, in which many reflection coefficients are constrained to be zero, have been proposed [54, 32]. *Conical* (rather than the usual cylindrical) tube segments and sparsely distributed *interpolating* scattering junctions have been proposed as further refinements [117, 115].

In musical sound synthesis and delay-effects applications, *digital waveguide models* have been used for *distributed* media, such as vibrating strings, bores, horns, plates, solids, acoustic spaces, and the like [93, 94, 97, 14, 15, 16, 18, 17, 36, 37, 103, 44, 46, 47, 8, 48, 98, 123, 119, 126, 116, 124, 115, 118, 120, 130, 6, 23, 49, 82, 121, 41, 73, 68, 100, 45, 77, 86, 87, 107, 85, 74, 101, 102, 30]. A digital waveguide is typically defined as a *bidirectional delay line* containing *sampled traveling waves*. This paper is concerned with general properties of digital waveguide models.

Digital waveguide models often include *lumped* elements such as masses and springs. Lumped element modeling is the main focus of *wave digital filters* (WDF) as developed principally by Fettweis [26, 27]. Wave digital filters derive from a scattering-theoretic formulation [4] and bilinear transformation [65] of *lumped* RLC elements. The formal traveling-wave signals in the scattering-theoretic description of lumped circuit elements are known as *wave variables*. Interfacing to digital waveguide models is simple since both use scattering-theoretic formulations. In acoustic modeling applications, WDFs can provide digital filters which serve as explicit physical models of mass, spring, and dashpot elements, as well as more exotic elements from classical network theory such as transformers, gyrators, and circulators. An example of using a WDF to model a nonlinear mass-spring system is the "wave digital piano hammer" [127]. For realizability of lumped models with feedback, wave digital filters also incorporate short waveguide sections called "unit elements," but these are ancillary to the main development. The digital waveguide formulation is actually more closely related to "unit element filters" which were developed much earlier than WDFs in microwave engineering [72].

Vaidyanathan and Mitra [113] developed a class of digital filters containing both the WDFs and the Gray-Markel normalized ladder structures [35], and proved low passband sensitivity to coefficient quantization and the absence of limit cycles, even under time-varying conditions. The generalized filter structure in [113] can itself be interpreted as a DWN consisting of a single *normalized* scattering junction (see Section 4) joining an input/output port and N waveguides which are each $1/2$ sample long and reflectively terminated at their other end.

Vaidyanathan and Mitra also defined a general family of *multivariable* digital ladder filters [112] and derived a synthesis procedure for m-input k-output transfer-function matrices based on recursive extraction of generalized scattering junctions from an allpass transfer-function matrix in which the desired transfer function is embedded. Each "vector" scattering junction is an elegant generalization of that in the Gray-Markel normalized ladder filter [57]. The extraction approach starts from the specification of a $k \times m$ matrix fraction description [43] of the desired allpass matrix and proceeds directly in the z domain.

Digital waveguide models, in contrast to WDFs and generalized Gray-Markel ladder filters, are typically derived directly from the geometry and physical properties of a desired acoustic system.

They are often used to simulate nearly lossless distributed vibrating structures such as strings, tubes, rods, membranes, plates, and so on, but only up to a certain bandwidth (the limit of human hearing in audio applications). In many cases we do not want simply to implement a transfer function; we need instead a complete *model* with which we can interact in a physically consistent way, even when parameters are time-varying and nonlinearities are introduced. In such cases, digital waveguide networks can provide a solid foundation.

1.2 Digital Waveguide Networks (DWN)

Wave propagation in distributed physical systems can be efficiently simulated using DWNs. The simplest case is a single bidirectional delay line which simulates wave propagation in a lossless cylindrical acoustic tube or ideal vibrating string [97] (see Fig. 1). A slightly more complex case is the cascade connection of two or more bidirectional delay lines, interconnected by two-port lossless scattering junctions, as in the Kelly-Lochbaum vocal-tract model (see Fig. 5, allpass section).

Terminating a cascade of bidirectional delay lines with an infinite or zero impedance yields total reflection from the termination (far left or far right in Fig. 5). In this case, delay elements for sampled signals traveling toward the termination can be *commuted* through the scattering junctions and combined with the delay elements for signals traveling away from the termination, and the sampling rate can be lowered by a factor of two [92]. This derives the ladder digital filter structure used in more modern speech coding via linear prediction [57]. Extending this procedure, the multivariable digital lattice filters synthesized according to [112] can be transformed via elementary delay manipulations to a multivariable DWN.

Wave propagation in *membranes* and *volumes* can be efficiently simulated using a *waveguide mesh* which is a grid of bidirectional delay lines interconnected by N-port lossless scattering junctions [93, 122, 84, 125, 30]. Highly efficient, multiply-free, lossless meshes can be obtained when the number of waveguides intersecting at each junction is a power of two [91]; this happens in the simple rectilinear 2D mesh, and also in the tetrahedral 3D mesh (analogous to the diamond crystal lattice) [125]. The common feature of DWNs is sampled unidirectional traveling waves in distributed wave-propagation media.

Digital waveguide networks (as well as WDFs or any digital filter with a physical interpretation) can be regarded as a special case of *finite difference methods* (FDM) [109]. Normally, FDMs are derived directly from differential equations by replacing differentials (dx, dt, etc.) by finite steps (Δx, Δt, etc.). A major distinction of DWN-induced FDMs is their inherent *stability*. Since DWNs for lossless media are by construction lossless networks of lossless sampled transmission lines, the stability problems normally associated with FDMs are avoided at the outset. Moreover, *dispersion* is often avoided completely in the 1D case, and it can be controlled from a different perspective in higher dimensions [124]. These advantages are quite useful in acoustic modeling applications which involve large-order systems which are very close to lossless (such as a vibrating string, plate, or reverberating chamber).

To incorporate linear propagation distortions (frequency-dependent attenuation and dispersion), recursive digital filters are typically embedded in the DWN at specific points. Rather than implement attenuation and dispersion in a uniformly sampled, distributed fashion (i.e., a small amount of filtering between each pair of unit-delay elements), one digital filter will normally implement the attenuation and dispersion associated with a much larger section of medium [97]. In principle, the required filter order increases with the size of the section being "summarized," but in nearly lossless media such as strings and acoustic tubes, the filtering per unit length of medium is so weak

that very low-order filters give very good approximations to many samples worth of wave propagation. This "lumping" of losses and dispersion in the discrete-time simulation can yield enormous complexity reductions, but it is also a source of approximation error which must be considered in the context of the application. In acoustic modeling over audio bandwidths, approximations of this kind are normally inaudible so long as the overall decay rates and tunings of the modes of the structure being modeled are preserved.

1.3 Properties of DWNs

Each delay element of a DWN can be interpreted precisely as a sampled traveling-wave component in a physical system, unlike the delay elements in ladder and lattice digital filters. Due to the particular bilinear-transform frequency warping used in typical WDFs, the delay elements in WDFs can be precisely interpreted as containing samples of physical traveling waves at dc, $f_s/4$, and $f_s/2$, where f_s denotes the sampling rate.

Because simple sampling of traveling waves is used to define DWNs, *aliasing* can occur if the bandwidths of the physical signals become too large, or if nonlinearities or time-varying parameters create signal components at frequencies above the Nyquist limit. (The bilinear transform, on the other hand, does not alias.) An advantage of simple sampling is that the *frequency axis is preserved exactly* up to half the sampling rate, while in the case of the bilinear transform, the frequency axis is warped so that only dc, $f_s/2$ and one other frequency can be mapped across exactly.

Due to the precise physical interpretation of DWNs, nonlinear and time-varying extensions are well behaved and tend to remain "physical", provided aliasing is controlled. (See Section 6.)

Because delay elements appear in physically meaningful locations in both the forward and reverse signal paths of a DWN, there is no restriction to a reflectively terminated cascade chain of scattering junctions as is normal in the ladder/lattice filter context. Digital waveguides can be coupled at junctions, cascaded, looped, or branched, to any degree of network complexity. As a result, much more general network topologies are available, corresponding to arbitrary physical constructions.

Lumped elements can be integrated into DWNs and results from WDF theory can be used to model both linear and nonlinear lumped circuit elements [58, 127, 21].

The instantaneous power anywhere in a DWN can be made invariant with respect to time-varying filter coefficients, as discussed in Sections 4 and 5. This can be seen as generalizing the normalized ladder filter [35, 92, 95].

As a result of the strict passivity which follows directly from the physical interpretation, no instability, limit cycles, or overflow oscillations can occur, even in the time-varying case, as long as "passive scattering" is used at all waveguide junctions [113, 92]. As explained in Section 6, passive scattering may be trivially obtained simply by using extended internal precision in each junction followed by magnitude truncation of all outgoing waves leaving the junction. However, in scattering intensive applications such as the 2D and 3D mesh, magnitude truncation often yields too much damping due to round-off, and more refined schemes must be used.

The basic characteristics of DWNs can be summarized as follows [95]:

- DWNs are derived by sampling traveling-wave descriptions of *distributed* physical wave-propagation systems such as strings, acoustic tubes, plates, gases, and solids.
- Each delay element of a DWN has a precise *physical interpretation* as a sample of a unidirectional traveling wave.

- The frequency axis is preserved up to half the sampling rate (i.e., it is not warped according to the bilinear transform).
- Physically meaningful *nonlinear, time-varying* extensions are straightforward.
- *Aliasing* can occur due to nonlinearities, time variation, or inadequate bandlimiting of initial conditions and/or input signals.
- Fully general modeling geometries are available (e.g., in contrast to ladder/lattice filters).
- Lumped models can be simply interfaced to DWNs.
- Overall signal energy can be simply controlled.
- Instability, limit cycles, can overflow oscillations can be suppressed by using "*passive* scattering."
- Sensitivity to coefficient quantization can be minimized.
- A *synthesis* procedure exists for constructing any single-input, single-output (SISO) transfer function by means of a DWN [111], and any m-input, k-output transfer function by means of a multivariable DWN [112].

1.4 Paper Outline

Section 2 gives a generalized formulation of waveguide models: After a short introduction in classical terms, we consider the m-component dual variables $\boldsymbol{p}$ and $\boldsymbol{u}$, which can be associated with any physical wave quantities such as acoustic pressure and volume velocity, or voltage and current. This discrete-time multivariable formulation, while leading to results similar to those in classical electrical network theory [4], provides a general framework giving a unified treatment of various modeling problems.

In Section 3, we define the lossless junction of waveguide sections in terms of energy conservation. Such a formulation yields a class of lossless scattering junctions larger than that arising from the set of all physically meaningful scattering junctions.

Section 4 discusses power normalization of waveguide variables, and the results are applicable to both physical and non-physical scattering junctions.

In Section 5, we summarize formulas for physical, normalized, and unnormalized scattering junctions of m-variable waveguide branches. We show how these junctions can be loaded with a lumped network and present an example in acoustic modeling.

In Section 6, using the physical interpretation of the computations, we give conditions for ensuring passivity of nonlinear and time-varying DWNs.

In Section 7, we present an algebraic analysis of the lossless junction, and the fundamental condition of losslessness is translated into the domain of eigenvalues and eigenvectors of the scattering matrix.

Section 8 shows how physical junctions can be implemented efficiently, both in the normalized and unnormalized cases. As a byproduct, two new three-multiply, three-add normalized lattice sections are derived. It is shown that the proposed implementations are robust with respect to coefficient quantization, and dynamic range requirements are addressed.

Section 9 considers an abstract geometric (as opposed to physically geometric) interpretation of physical scattering computations. The normalized scattering matrix is shown to be equivalent to a Householder reflection, while the unnormalized case can be seen as an oblique Householder reflection. Householder matrices are highly valued in numerical analysis because they conserve numerical dynamic range and thereby yield robust algorithms [34]. As a byproduct of this viewpoint, another new three-multiply, three-add normalized lattice section is derived which is especially well suited for implementation on general-purpose digital signal processing chips.

For completeness, Section 10 briefly covers the extension of lossless scattering and junction normalization to the case in which scattering matrices may contain complex rational transfer function elements. Such cases arise in the computational modeling of acoustic systems such as intersecting conical tubes and woodwind fingerholes. Junctions loaded by an arbitrary lumped impedance (e.g., a Helmholtz resonator mouthpiece model or complex violin bridge impedance), can also be handled this way.

2 Basic DWN Formulation

This section reviews the DWN paradigm and briefly outlines considerations arising in acoustic simulation applications.

The formulation is based on dual m-dimensional vectors of "pressure" and "velocity" $\boldsymbol{p}$ and $\boldsymbol{u}$, respectively. These variables can be associated with acoustic pressure and particle- or volume-velocity, or they can be anything analogous such as electrical voltage and current, mechanical force and velocity, etc. We call these dual variables *Kirchhoff variables* to distinguish them from *wave variables* which are their traveling-wave components. For concreteness, we will focus on pressure and velocity waves in a lossless, linear, *acoustic tube*. In acoustic tubes, velocity waves are in units of volume velocity (particle velocity times the tube cross-sectional area) [60].

2.1 The Ideal Acoustic Tube

First we address the scalar case. For an ideal acoustic tube, we have the following *wave equation* [60]:

$$\frac{\partial^2 p(x,t)}{\partial t^2} = c^2 \frac{\partial^2 p(x,t)}{\partial x^2} \tag{1}$$

where $p(x,t)$ denotes (scalar) pressure in the tube at the point x along the tube at time t in seconds. If the length of the tube is L_R, then x is taken to lie between 0 and L_R. We adopt the convention that x increases "to the right" so that waves traveling in the direction of increasing x are referred to as "right-going." The constant c is the speed of sound propagation in the tube, given by $c = \sqrt{K/\mu}$, where K is the "spring constant" or "stiffness" of the air in the tube,[2] and μ is the mass per unit volume of the tube. The dual variable, volume velocity u, also obeys (1) with p replaced by u. The wave equation (1) also holds for an ideal string, if p represents the transverse displacement, K is the tension of the string, and μ is its linear mass density.

The wave equation (1) follows from the more physically meaningful *telegrapher's equations* [24]:

$$-\frac{\partial p(x,t)}{\partial x} = \mu \frac{\partial u(x,t)}{\partial t} \tag{2}$$

[2] "Stiffness" is defined here for air as the reciprocal of the adiabatic compressibility of the gas [61, p. 230]. This definition helps to unify the scattering formalism for acoustic tubes with that of mechanical systems such as vibrating strings.

$$-\frac{\partial u(x,t)}{\partial x} \quad = \quad K^{-1}\frac{\partial p(x,t)}{\partial t} \tag{3}$$

Equation (2) follows immediately from Newton's second law of motion, while (3) follows from conservation of mass and properties of an ideal gas [61].

The general traveling-wave solution to (1), (2), and (3) was given by D'Alembert [60] as

$$\begin{aligned} p(x,t) &= p^+(x-ct) + p^-(x+ct) \\ u(x,t) &= u^+(x-ct) + u^-(x+ct) \end{aligned} \tag{4}$$

where p^+, p^-, u^+, u^- are the right- and left-going wave components of pressure and velocity, respectively, and are referred to as *wave variables*. This solution form is interpreted as the sum of two fixed wave-shapes traveling in opposite directions along the uniform tube. The specific wave-shapes are determined by the initial pressure $p(x,0)$ and velocity $u(x,0)$ throughout the tube for $x \in [0, L_R]$.

2.2 Multivariable Formulation of the Acoustic Tube

A straightforward multivariable generalization of the telegrapher's equations (2) and (3) gives the following m-variable generalization of the wave equation (5):

$$\frac{\partial^2 \boldsymbol{p}(\boldsymbol{x},t)}{\partial t^2} = \boldsymbol{K}\boldsymbol{M}^{-1}\frac{\partial^2 \boldsymbol{p}(\boldsymbol{x},t)}{\partial \boldsymbol{x}^2} \tag{5}$$

in the spatial coordinates $\boldsymbol{x}^T \stackrel{\triangle}{=} \left[\begin{array}{ccc} x_1 & \ldots & x_m \end{array}\right]$ at time t, where $\boldsymbol{M}$ and $\boldsymbol{K}$ are $m \times m$ non-singular, non-negative matrices which play the respective roles of multidimensional mass and stiffness. The second spatial derivative is defined here as

$$\left[\frac{\partial^2 \boldsymbol{p}(\boldsymbol{x},t)}{\partial \boldsymbol{x}^2}\right]^T \stackrel{\triangle}{=} \left[\begin{array}{ccc} \frac{\partial^2 p_1(\boldsymbol{x},t)}{\partial x_1^2} & \ldots & \frac{\partial^2 p_m(\boldsymbol{x},t)}{\partial x_m^2} \end{array}\right] \tag{6}$$

For digital waveguide modeling, we desire solutions of the multivariable wave equation which involve only sums of traveling waves, because traveling wave propagation can be efficiently simulated digitally using only delay lines, digital filters, and scattering junctions. Consider the eigenfunction

$$\boldsymbol{p}(\boldsymbol{x},t) = \left[\begin{array}{l} e^{st+v_1x_1} \\ \ldots \\ e^{st+v_mx_m} \end{array}\right] \stackrel{\triangle}{=} e^{st\boldsymbol{I}+\boldsymbol{V}\boldsymbol{X}} \cdot \boldsymbol{1} \tag{7}$$

where s is interpreted as a Laplace-transform variable $s = \sigma + j\omega$, $\boldsymbol{I}$ is the $m \times m$ identity matrix, $\boldsymbol{X} \stackrel{\triangle}{=} \mathrm{diag}(\boldsymbol{x})$, $\boldsymbol{V} \stackrel{\triangle}{=} \mathrm{diag}([v_1, \ldots, v_m])$ is a diagonal matrix of *spatial* Laplace-transform variables (the imaginary part of v_i being spatial frequency along the ith spatial coordinate), and $\boldsymbol{1}^T \stackrel{\triangle}{=} [1, \ldots, 1]$. Substituting the eigenfunction (7) into (5) gives the algebraic equation

$$s^2\boldsymbol{I} = \boldsymbol{K}\boldsymbol{M}^{-1}\boldsymbol{V}^2 \stackrel{\triangle}{=} \boldsymbol{C}^2\boldsymbol{V}^2 \tag{8}$$

where $\boldsymbol{C}$ is the diagonal matrix of sound-speeds along the m coordinate axes. Since $\boldsymbol{C}^2\boldsymbol{V}^2 = s^2\boldsymbol{I}$, we have

$$\boldsymbol{V} = \pm s\boldsymbol{C}^{-1}. \tag{9}$$

Substituting (9) into (7), the eigensolutions of (5) are found to be of the form

$$\boldsymbol{p}(\boldsymbol{x},t) = e^{s\left(t\boldsymbol{I}\pm\boldsymbol{C}^{-1}\boldsymbol{X}\right)}\cdot\boldsymbol{1} \tag{10}$$

Having established that (10) is a solution of (5) when condition (8) holds for the matrices $\boldsymbol{M}$ and $\boldsymbol{K}$, we can express the general traveling-wave solution to (5) in both pressure and velocity as

$$\begin{aligned}\boldsymbol{p}(\boldsymbol{x},t) &= \boldsymbol{p}^+ + \boldsymbol{p}^-\\ \boldsymbol{u}(\boldsymbol{x},t) &= \boldsymbol{u}^+ + \boldsymbol{u}^-\end{aligned} \tag{11}$$

where $\boldsymbol{p}^+ \stackrel{\triangle}{=} f(t\boldsymbol{I}-\boldsymbol{C}^{-1}\boldsymbol{X})$, with f being an arbitrary superposition of right-going components of the form (10) (i.e., taking the minus sign), and $\boldsymbol{p}^- \stackrel{\triangle}{=} g(t\boldsymbol{I}+\boldsymbol{C}^{-1}\boldsymbol{X})$ is similarly any linear combination of left-going eigensolutions from (10) (all having the plus sign). Similar definitions apply for $\boldsymbol{u}^+$ and $\boldsymbol{u}^-$. When the time and space arguments are dropped as in the right-hand side of (11), it is understood that all the quantities are written for time t and position $\boldsymbol{x}$.

When the mass and stiffness matrices $\boldsymbol{M}$ and $\boldsymbol{K}$ are diagonal, our analysis corresponds to considering m separate waveguides as a whole. For example, the three directions of vibration (one longitudinal and two transverse) in a single terminated string can be described by (5) with $m = 3$. The coupling among the strings occurs primarily at the bridge in a piano [132]. As we will see later, the bridge acts like a junction of several multivariable waveguides.

When the matrices $\boldsymbol{M}$ and $\boldsymbol{K}$ are non-diagonal, the physical interpretation can be of the form

$$\boldsymbol{C}^2 \stackrel{\triangle}{=} \boldsymbol{K}\boldsymbol{M}^{-1} \tag{12}$$

where $\boldsymbol{K}$ is the *stiffness matrix,* $\boldsymbol{M}$ is the *mass density matrix.* $\boldsymbol{C}$ is diagonal if (8) holds, and in this case, the wave equation (5) is decoupled in the spatial dimensions. There are physical examples where the matrices $\boldsymbol{M}$ and $\boldsymbol{K}$ are not diagonal, even though $\boldsymbol{C}^2 \stackrel{\triangle}{=} \boldsymbol{K}\boldsymbol{M}^{-1}$ is. One such example, in the domain of electrical variables, is given by m conductors in a sheath or above a ground plane, where the sheath or the ground plane acts as a coupling element [63, pp. 67–68].

Note that the multivariable wave equation (5) considered here does not include wave equations governing propagation in multidimensional media (such as membranes, spaces, and solids). In higher dimensions, the solution in the ideal linear lossless case is a superposition of waves traveling in *all directions* in the m-dimensional space [60]. However, it turns out [122] that a good simulation of wave propagation in a multidimensional medium may be in fact be obtained by forming a *mesh* of unidirectional waveguides as considered here, each described by (5). Such a mesh of 1D waveguides can be shown to solve numerically a discretized wave equation for multidimensional media [125].

2.3 Generalized Wave Impedance

From the multivariable generalization of (2), we have, using (10), $\partial\boldsymbol{p}(\boldsymbol{x},t)/\partial\boldsymbol{x} = -\boldsymbol{M}\partial\boldsymbol{u}(\boldsymbol{x},t)/\partial t \Rightarrow \pm s\boldsymbol{C}^{-1}\boldsymbol{p} = -s\boldsymbol{M}\boldsymbol{u} \Rightarrow \boldsymbol{p} = \pm\boldsymbol{C}\boldsymbol{M}\boldsymbol{u} = \pm\boldsymbol{K}^{1/2}\boldsymbol{M}^{1/2}\boldsymbol{u} \stackrel{\triangle}{=} \pm\boldsymbol{R}\boldsymbol{u}$, where '+' is for right-going and '−' is for left-going. Thus, following the classical definition for the scalar case, the *wave impedance* is defined by

$$\boldsymbol{R} \stackrel{\triangle}{=} \boldsymbol{K}^{1/2}\boldsymbol{M}^{1/2} = \boldsymbol{C}\boldsymbol{M}$$

and we have

$$\begin{aligned} \boldsymbol{p}^+ &= \boldsymbol{R}\boldsymbol{u}^+ \\ \boldsymbol{p}^- &= -\boldsymbol{R}\boldsymbol{u}^- \end{aligned} \tag{13}$$

Thus, the wave impedance $\boldsymbol{R}$ is the factor of *proportionality* between pressure and velocity in a traveling wave. It is diagonal if and only if the mass matrix $\boldsymbol{M}$ is diagonal (since $\boldsymbol{C}$ is assumed diagonal). The minus sign for the left-going wave $\boldsymbol{p}^-$ accounts for the fact that velocities must move to the left to generate pressure to the left. The *wave admittance* is defined as $\boldsymbol{\Gamma} = \boldsymbol{R}^{-1}$.

More generally, when there is a loss represented by a diagonal matrix $\boldsymbol{G}$, we have, in the continuous-time case,

$$\boldsymbol{p} = e^{\boldsymbol{G}\boldsymbol{X}} e^{s\left(t\boldsymbol{I} - \boldsymbol{C}^{-1}\boldsymbol{X}\right)} \cdot \boldsymbol{1} \tag{14}$$

where $\boldsymbol{X} \stackrel{\triangle}{=} \mathrm{diag}(\boldsymbol{x})$ as before, leading to the admittance matrix

$$\boldsymbol{\Gamma} = \boldsymbol{M}^{-1}\boldsymbol{C}^{-1} - \frac{1}{s}\boldsymbol{M}^{-1}\boldsymbol{G} \tag{15}$$

For the discrete-time case, we may map $\boldsymbol{\Gamma}(s, \boldsymbol{x})$ from the s plane to the z plane via the bilinear transform [65], or we may sample the inverse Laplace transform of $\boldsymbol{\Gamma}(s, \boldsymbol{x})$ and take its z transform to obtain $\hat{\boldsymbol{\Gamma}}(z, \boldsymbol{x})$.

A linear propagation medium in the discrete-time case is completely determined by its *wave impedance* $\boldsymbol{R}(z, \boldsymbol{x})$ (generalized here to permit frequency-dependent and spatially varying wave impedances). A *waveguide* is defined for purposes of this paper as a length of medium in which the wave impedance is either constant with respect to spatial position x, or else it varies smoothly with x in such a way that there is no scattering (as in the conical acoustic tube). For simplicity, we will suppress the possible spatial dependence and write only $\boldsymbol{R}(z)$.[3]

2.4 Generalized Complex Signal Power

The *net complex power* involved in the propagation can be defined as [4]

$$\begin{aligned} \mathcal{P} &= \boldsymbol{u}^*\boldsymbol{p} = (\boldsymbol{u}^+ + \boldsymbol{u}^-)^*(\boldsymbol{p}^+ + \boldsymbol{p}^-) \\ &= \boldsymbol{u}^{+*}\boldsymbol{R}\boldsymbol{u}^+ - \boldsymbol{u}^{-*}\boldsymbol{R}^*\boldsymbol{u}^- + \\ &\quad \boldsymbol{u}^{-*}\boldsymbol{R}\boldsymbol{u}^+ - \boldsymbol{u}^{+*}\boldsymbol{R}^*\boldsymbol{u}^- \\ &\stackrel{\triangle}{=} (\mathcal{P}^+ - \mathcal{P}^-) + (\mathcal{P}^\times - \mathcal{P}^{\times *}) \end{aligned} \tag{16}$$

where all quantities above may be functions of z, and "$*$" denotes *paraconjugation* (transposition and complex conjugation on the unit circle in the z plane). The quantity $\mathcal{P}^+ = \boldsymbol{u}^{+*}\boldsymbol{R}\boldsymbol{u}^+$ is called *right-going active power* (or right-going average dissipated power[4]), while $\mathcal{P}^- = \boldsymbol{u}^{-*}\boldsymbol{R}^*\boldsymbol{u}^-$

[3] There are no tube shapes supporting exact traveling waves other than cylindrical and conical (or conical wedge, which is a hybrid) [69]. However, the "Salmon horn family" (see, e.g., [60, 96]) characterizes a larger class of *approximate* "one-parameter traveling waves." In the cone, the wave equation is solved for pressure $p(x,t)$ using a change of variables $p' = px$, where x is the distance from the apex of the cone, causing the wave equation for the cone to reduce to that of the cylindrical case [2].

[4] Note that $|z| = 1$ corresponds to the average physical power at frequency ω, where $z = \exp(j\omega T)$, and the wave variable magnitudes on the unit circle may be interpreted as RMS levels [4, p. 48]. For $|z| > 1$, we may interpret the power $\mathcal{P}(z) = \boldsymbol{u}^*(1/z^*)\boldsymbol{p}(z)$ as the steady state power obtained when exponential damping is introduced into the waveguide giving decay time-constant τ, where $z = \exp(-T/\tau)\exp(j\omega T)$ [4, p. 48].

is called the *left-going active power*. The term $\mathcal{P}^+ - \mathcal{P}^-$, the right-going minus the left-going power components, we call the *net active power*, while the term $\mathcal{P}^\times - \mathcal{P}^{\times *}$ is *net reactive power*. These names all stem from the case in which the matrix $\boldsymbol{R}(z)$ is positive definite for $|z| \geq 1$. In this case, both traveling components of the active power are real and positive, the active power itself is real, and the reactive power is purely imaginary.

2.5 Medium Passivity

Following the classical definition of passivity [4, 133], a medium is said to be *passive* if

$$\mathcal{P}^+ + \mathcal{P}^- \geq 0 \tag{17}$$

for $|z| \geq 1$. Thus, a sufficient condition for ensuring passivity in a medium is that each traveling active-power component be real and non-negative.

To derive a definition of passivity in terms of the wave impedance, consider a perfectly reflecting interruption in the transmission line, such that $\boldsymbol{u}^- = \boldsymbol{u}^+$. For a passive medium, using (16), (17) becomes

$$\boldsymbol{R}(z) + \boldsymbol{R}^*(1/z^*) \geq 0 \tag{18}$$

for $|z| \geq 1$. The wave impedance $\boldsymbol{R}(z)$ is an m-by-m function of the complex variable z. Condition (18) is essentially the same thing as saying $\boldsymbol{R}(z)$ is *positive real* [128], except that it is allowed to be complex (but Hermitian), even for real z.[5] The matrix $\boldsymbol{R}^*(1/z^*)$ is the paraconjugate of $\boldsymbol{R}$, i.e., the unique analytic continuation (when it exists) of the Hermitian transpose of $\boldsymbol{R}$ from the unit circle to the complex z plane [110]. Since the inverse of a positive-real function is positive real, the corresponding generalized wave admittance $\boldsymbol{\Gamma}(z) = \boldsymbol{R}^{-1}(z)$ is positive real (and hence analytic) in $|z| \geq 1$. In other terms, the sum of the wave impedance and its paraconjugate is positive semidefinite.

We say that wave propagation in the medium is *lossless* if the wave impedance matrix satisfies

$$\boldsymbol{R}(z) = \boldsymbol{R}^*(1/z^*) \tag{19}$$

i.e., if $\boldsymbol{R}(z)$ is para-Hermitian (which implies its inverse $\boldsymbol{\Gamma}(z)$ is also).

Most applications in waveguide modeling are concerned with nearly lossless propagation in passive media. In this paper, we will state results for $\boldsymbol{R}(z)$ in the more general case when applicable, while considering applications only for constant and diagonal impedance matrices $\boldsymbol{R}$. As shown in Section 2.3, coupling in the wave equation (5) implies a non-diagonal impedance matrix, since there is usually a proportionality between the speed of propagation $\boldsymbol{C}$ and the impedance $\boldsymbol{R}$ through the non-diagonal matrix $\boldsymbol{M}$.

The wave components of equations (11) travel undisturbed along each axis. This propagation is implemented digitally using m *bidirectional delay lines*, as depicted in Fig. 1. We call such a collection of delay lines an m*-variable waveguide section*. Waveguide sections are then joined at their endpoints via *scattering junctions* (discussed further in following sections) to form a DWN.

[5] A complex-valued function of a complex variable $f(z)$ is said to be *positive real* if

1) z real $\Rightarrow$ $f(z)$ real

2) $|z| \geq 1 \Rightarrow \mathrm{Re}\{f(z)\} \geq 0$

Positive real functions characterize passive impedances in classical network theory [129].

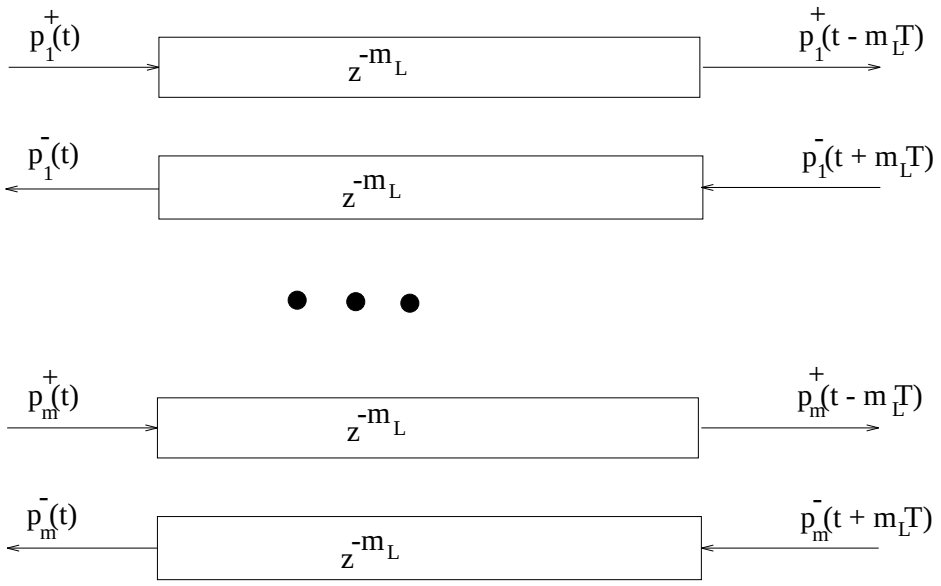

Figure 1: An m-variable waveguide section.

2.6 Impulsive Signals Interpretation

Let c denote the speed of propagation in one branch of an m-variable waveguide section having real, positive wave impedance $\boldsymbol{R}$. Let L be the linear length of this branch in samples. The propagation time from one end to the other is $T_p = L/c$. If $T_p = nT$, where T is the sampling interval of the digital network, the (frequency-independent) propagation in the branch can be precisely simulated (ignoring any roundoff errors due to scattering at the endpoints). Extending this restriction to every branch in the network, we can state that a DWN is equivalent to a physical waveguide network in which the input pressure signals are streams of weighted impulses at intervals of T seconds. This equivalence is also true in the case of time-varying wave impedances. The impulsive nature of the propagating signals serves to sample the junction scattering coefficients at the digital sampling instants.

2.7 Bandlimited Signals Interpretation

A more practically useful correspondence between physical and digital waveguide networks is obtained by assuming the inputs to the physical networks are bandlimited continuous-time Kirchoff variables. The signals propagating throughout the physical network are assumed to consist of frequencies less than $f_s/2$ Hz, where $f_s = 1/T$ denotes the sampling rate. Therefore, by the Shannon sampling theorem, if we record a sample of the pressure wave, say, at each unit-delay element every T seconds, the bandlimited continuous pressure fluctuation can be uniquely reconstructed throughout the waveguide network. Saying the pressure variation is frequency bandlimited to less than $f_s/2$ is equivalent to saying the pressure distribution is spatially bandlimited to less than $f_s/2c$, or, a one-sample section of waveguide is less than half a cycle of the shortest wavelength contained in a traveling wave. In summary, a DWN is equivalent to a physical waveguide network in which the input signals are bandlimited to $f_s/2$ Hz. This equivalence does not remain true for time-varying or non-linear DWNs.

In the case of time-varying wave impedances, the time-variation of the resultant scattering coefficients applies a continuous amplitude modulation to the continuous propagating signals, thereby generating sidebands. If the signals incident on a junction are bandlimited to f_1 Hz and the scattering coefficients are bandlimited to f_2 Hz, then the signals emerging from an interconnection of waveguides are bandlimited only to $f_1 + f_2$ Hz. If the network is nontrivial, a portion of the amplitude-modulated signals may return to the same time-varying junction, and the signal bandwidth expands to $f_1 + 2f_2$, and so on. A time-varying junction eventually expands the bandwidth of the signals contained in the network to infinity. With a fixed sampling rate f_s in the DWN, we obtain *aliased* versions of the physical signals. The general result is that time-varying physical waveguide networks cannot be simulated by DWNs at a fixed sampling rate. In practice, however, we obtain good *approximate* digital simulations by working with wave variables and junction parameters bandlimited to much less than $f_s/2$, and by using sufficient damping (implemented using low-pass filtering) in the network so that the aliased signal energy is attenuated below significance.

Particular care must be used also when inserting nonlinear elements into waveguide networks, since they also extend the bandwidth, and frequency foldover will result. Nonlinear elements are almost always present in the excitation blocks of musical instruments (e.g., reeds, bows, and felt-covered hammers), sometimes also in the resonators (e.g., brasses, sitar strings and cymbals), and sometimes also in the output amplification/diffusion stage (e.g., a saturating amplifier or speaker simulation). Nonlinearities in the resonators (such as a sitar string) may be sufficiently weak so that inherent low-pass filtering can attenuate nonlinearly generated high frequencies to insignificance before they alias. Also, nonlinear excitations can be bandlimited using a lowpass filter if they are not strongly coupled to the resonator they excite (the "source-filter" decomposition). Similarly, nonlinearities in the output path can be implemented without aliasing in the absence of feedback to the resonator or excitation. In some practical cases, conditions for the passivity of nonlinearities can be determined [127, 62, 81]. However, preventing aliasing is much more difficult. One strategy is to use low-order polynomials to implement nonlinearities. A polynomial of order n expands the bandwidth by only a factor of n. Therefore, bandlimiting the nonlinearity input to $f_s/(2n)$ and oversampling by a factor of n will avoid aliasing.

A third reason (beyond time-variation and nonlinearity support) for adopting a sampling rate significantly higher than the audio frequency bandwidth is the necessity of using *fractional delays*. These are needed whenever a high spatial resolution is needed, or when the waveguide length must be "continuously" variable. In all these cases digital interpolators must be used, in the form of FIR or IIR filters, ideally allpass (see next subsection). To some extent, both FIR and IIR filter types introduce amplitude and/or phase distortion at high frequencies, so it is typically beneficial to increase the sampling rate and provide a "guard band" between 20 kHz (for high fidelity audio) and $f_s/2$.

2.8 Interpolated Digital Waveguides

Integer delay lengths are not sufficient for musical tuning of digital waveguide models at commonly used sampling rates [40]. The simplest scheme which is typically tried first is *linear interpolation*. However, poor results are obtained in some cases (such electric guitar models) due to the pitch-dependent damping caused by delay-line interpolation. As is well known [88], linear interpolation is equivalent to a time-varying FIR filter of the form $y(n) = \alpha(n)x(n) + [1 - \alpha(n)]x(n - 1)$, and for $\alpha(n) = 0.5$ (for interpolation half way between available samples), the gain of the interpolation filter at $f_s/2$ drops to zero. In some cases, such as for steel string simulation, the interpolation filter

becomes the dominant source of damping, so that when the pitch happens to fall on an integer delay-line length ($\alpha = 0$), the damping suddenly decreases, making the note stand out as "buzzy." In such cases, something better than linear interpolation is required.

Allpass interpolation is a nice choice for the nearly lossless feedback loops commonly used in digital waveguide models [40, 104], because it does not suffer *any* frequency-dependent damping. Its phase distortion normally manifests as a slight mistuning of high-frequency resonances, which is usually inaudible and arguably even desirable in most cases. However, allpass interpolation instead has the problem that instantly switching from one delay to another (as in a "hammer-on" or "pull-off" simulation in a string model) gives rise to a *transient artifact* due to the recursive nature of the allpass filter. Transient artifacts can be reduced or eliminated by "warming up" a second instance of the filter using the new coefficients in advance of the transition (ideally several time-constants in advance) and, at the desired transition time, switching out the old filter and switching in the new [120]. In this way, the new filter is switched in with state consistent with the new coefficients. Another approach is to *cross-fade* from the old filter to the new filter, allowing consistent state to develop in the new filter before its output fades in.

Another popular choice is *Lagrange interpolation* [46, 115, 1, 88] which is a special case of FIR filter interpolation; while the transient artifact problem is minimal since the interpolating filter is nonrecursive, there is still a time-varying amplitude distortion at high frequencies. In fact, first-order Lagrange interpolation is just linear interpolation, and higher orders can be shown to give a maximally smooth frequency response at dc (zero frequency), while the gain generally rolls off at high frequencies. Allpass interpolation can be seen as trading off this frequency-dependent amplitude distortion for additional frequency-dependent delay distortion [13]. A comprehensive review of Lagrange interpolation appears in [115].

Both allpass and FIR interpolation suffer from some delay distortion at high frequencies due to having a nonlinear phase response at non-integer desired delays. As mentioned above for the allpass case alone, this distortion is normally inaudible, even in the first-order case, causing mistuning or phase modulation only in the highest partial overtones of a resonating string or tube.

Optimal interpolation can be approached via general-purpose *bandlimited interpolation* techniques [105, 70]. However, the expense is generally considered too high for widespread usage at present. Both amplitude and delay distortions can be eliminated over the entire band of human hearing using higher order IIR (e.g., allpass) or FIR interpolation filters in conjunction with some amount of oversampling. A comprehensive review of delay-line interpolation techniques is given in [53].

2.9 Lossy, Dispersive Waveguides

In reality, distributed linear propagation is never lossless. There is always some attenuation and dispersion per unit distance traveled by a wave in the medium. In principle, implementing loss and dispersion calls for a digital filter to be inserted at the output of every delay element to precisely simulate one sample of wave propagation. In practice this is generally unnecessary. Instead, we may normally implement digital filters *sparsely* along each digital waveguide [97, 99]. Each filter provides the attenuation and dispersion corresponding to the propagation distance over the section it covers. In other words, lossy, dispersive media are approximated by *piecewise lossless* media having the same average attenuation and dispersion over long distances. Loss and dispersion are thus *lumped* at sparse points along the waveguide model rather than being lumped at each spatial sampling point.

In the 1D case, it is possible to obtain exact results using sparsely lumped losses and dispersion, thanks to the *commutativity* of linear, time-invariant elements [99]. For example, consider an acoustic cylinder which is L samples long. If the per-sample traveling-wave filter is given by $H_s(z)$, and if we only care what happens at the endpoints of the tube, then we need only implement the filter $H_s^L(z)$ at each end of the L-sample tube, prior to any junctions. Since the per-sample filtering $H_s(z)$ is typically very weak, the stronger filter $H_s^L(z)$ is normally also quite weak and readily approximated to within audio specifications by a low-order digital filter.

It is easy to show that the per-sample traveling-wave filter $H_s(z)$ for any *passive* propagation medium such as a string or acoustic cylinder must satisfy $\left|H_s(e^{j\omega})\right| \leq 1$ for all $\omega \in [-\pi, \pi]$. That is, wave propagation in a fixed wave impedance cannot increase traveling-wave amplitude at any frequency. This is a convenient stability criterion which is straightforward to ensure in practice.

In summary, wave propagation in a general linear time-invariant medium is thus simulated using a (possibly interpolated) delay line to handle the time-delay associated with the propagation, and one or more digital filters to sparsely implement losses and dispersion where needed, such as prior to a bow-string contact model [90].

2.10 The General Linear Time-Invariant Case

Let $y(t,x)$ denote the transverse displacement, in one plane, of a vibrating string [60]. The complete linear time-invariant generalization of the lossy, stiff string is described by the differential equation

$$\sum_{k=0}^{\infty} \alpha_k \frac{\partial^k y(t,x)}{\partial t^k} = \sum_{l=0}^{\infty} \beta_l \frac{\partial^l y(t,x)}{\partial x^l}. \tag{20}$$

which, on setting $y(t,x) = e^{st+vx}$, (or taking the 2D Laplace transform with zero initial conditions), yields the algebraic equation,

$$\sum_{k=0}^{\infty} \alpha_k s^k = \sum_{l=0}^{\infty} \beta_l v^l. \tag{21}$$

Solving for v in terms of s is, of course, nontrivial in general. However, in specific cases, we can determine the appropriate attenuation per sample $G(\omega)$ and wave propagation speed $c(\omega)$ by numerical means. For example, starting at $s = 0$, we normally also have $v = 0$ (corresponding to the absence of static deformation in the medium). Stepping s forward by a small differential $j\Delta\omega$, the left-hand side can be approximated by $\alpha_0 + \alpha_1 j\Delta\omega$. Requiring the generalized wave velocity $s/v(s)$ to be continuous, a physically reasonable assumption, the right-hand side can be approximated by $\beta_0 + \beta_1 \Delta v$, and the solution is easy. As s steps forward, higher order terms become important one by one on both sides of the equation. Each new term in v spawns a new solution for v in terms of s, since the order of the polynomial in v is incremented. For each solution $v(s)$, let $v_r(\omega)$ denote the real part of $v(j\omega)$ and let $v_i(\omega)$ denote the imaginary part. Then the eigensolution family can be seen in the form $\exp\{j\omega t \pm v(j\omega)x\} = \exp\{\pm v_r(\omega)x\} \cdot \exp\{j\omega\,(t \pm v_i(\omega)x/\omega)\}$. Defining $c(\omega) \stackrel{\triangle}{=} \omega / v_i(\omega)$, and sampling according to $x \to x_m \stackrel{\triangle}{=} mX$ and $t \to t_n \stackrel{\triangle}{=} nT(\omega)$, with $X \stackrel{\triangle}{=} c(\omega)T(\omega)$, (the spatial sampling period is taken to be frequency invariant, while the temporal sampling interval is modulated versus frequency using allpass filters), the left- and right-going sampled eigensolutions become

$$\begin{aligned} e^{j\omega t_n \pm v(j\omega)x_m} &= e^{\pm v_r(\omega)x_m} \cdot e^{j\omega[t_n \pm x_m/c(\omega)]} \\ &= G^m(\omega) \cdot e^{j\omega(n\pm m)T(\omega)} \end{aligned} \tag{22}$$

where $G(\omega) \stackrel{\triangle}{=} e^{\pm v_r(\omega)X}$. Thus, a general map of v versus s, corresponding to a partial differential equation of any order in the form (20), can be translated, in principle, into an accurate, local, linear, time-invariant, discrete-time simulation. The boundary conditions and initial state determine the initial mixture of the various solution branches as is typical in, say, the stiff string [19].

In summary, a large class of wave equations with constant coefficients, of any order, admits a decaying, dispersive, traveling-wave type solution. Even-order time derivatives give rise to frequency-dependent dispersion and odd-order time derivatives correspond to frequency-dependent losses. Higher order spatial derivatives can be approximated by higher order time derivatives and treated similarly [10]. The corresponding digital simulation of an arbitrarily long (undriven and unobserved) section of 1D medium (such as a string or acoustic tube) can be simplified via commutativity to at most two pure delays and at most two linear, time-invariant filters. In higher dimensions, such as for the 2D mesh, the per-sample filtering cannot in general be exactly commuted to the boundaries of the mesh. However, an approximation problem can be solved which matches the observed modal frequencies and decay rates using sparsely distributed low-order filters in an otherwise lossless mesh (e.g., around the rim).

In practical physical simulation scenarios, such as for real-world strings or acoustic tubes, it is generally most effective to identify *experimentally* the attenuation and dispersion associated with wave propagation at each frequency over the band of interest [108, 49]. These data can be used to design a digital filter which gives an optimal approximation over the propagation distance desired. If needed, the per-sample filter identified in this way can be translated into higher-order terms in the wave equation for the medium. Thus, the wave equation itself can be "identified" from measured input-output behavior of the medium (assuming it is linear and uniform) rather than being derived from physical principles and physical constants of the medium as is classically done [61, 11].

3 The Lossless Junction

A scattering junction of waveguide sections is characterized by its *scattering matrix* $\boldsymbol{A}$. The relationship between the N incoming and outgoing traveling waves is given by:

$$\boldsymbol{p}^- = \boldsymbol{A}\boldsymbol{p}^+ \tag{23}$$

where $\boldsymbol{p}^+$ is the vector of incoming waves (assumed scalar here) and $\boldsymbol{p}^-$ is the vector of outgoing waves relative to the junction (see Fig. 2). We say that the junction is N-way (or it has N branches) if N is the dimension of the incoming and outgoing wave vectors.

We now consider the case of a constant scattering matrix $\boldsymbol{A}$. The more general case of scattering matrices as functions of z will be considered in Section 10.

The net complex power entering the junctions is

$$\begin{aligned}
\mathcal{P} = \boldsymbol{u}^*\boldsymbol{p} &= \boldsymbol{p}^{+*}\boldsymbol{\Gamma}^*(1/z^*)\boldsymbol{p}^+ - \boldsymbol{p}^{-*}\boldsymbol{\Gamma}\boldsymbol{p}^- + \\
&\quad \boldsymbol{p}^{+*}\boldsymbol{\Gamma}^*(1/z^*)\boldsymbol{p}^- - \boldsymbol{p}^{-*}\boldsymbol{\Gamma}\boldsymbol{p}^+ \\
&= (\mathcal{P}^+ - \mathcal{P}^-) + (\mathcal{P}^\times - \mathcal{P}^{\times *})
\end{aligned} \tag{24}$$

where $\boldsymbol{\Gamma}$ is the diagonal matrix containing the N wave admittances of all the branches meeting at the junction. Assuming the branch admittances are Hermitian and nonzero, we have that $\boldsymbol{\Gamma}$ has positive real elements along its diagonal and zeros elsewhere. The quantity $\mathcal{P}^+ = \boldsymbol{p}^{+*}\boldsymbol{\Gamma}\boldsymbol{p}^+ \geq 0$ is

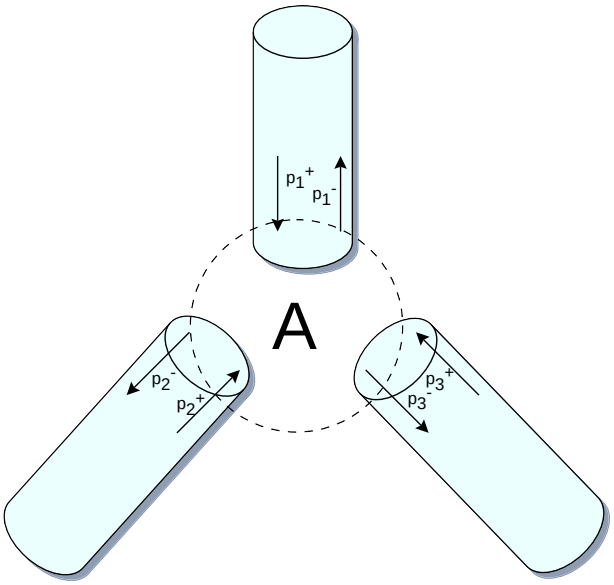

Figure 2: A schematic depiction of the 3-way waveguide junction.

incoming active power, and $\mathcal{P}^- = \boldsymbol{p}^{-*}\boldsymbol{\Gamma}\boldsymbol{p}^- \geq 0$ is then the *outgoing* active power relative to the junction. The term $\mathcal{P}^+ - \mathcal{P}^-$ is the *absorbed active power*, while the term $\mathcal{P}^\times - \mathcal{P}^{\times *}$, containing the mixed incoming and outgoing waves, is called the *reactive power*.

A scattering junction is said to be *passive* when the absorbed active power is nonnegative, i.e., when

$$\mathcal{P}^+ \geq \mathcal{P}^- \tag{25}$$

for $|z| \geq 1$. In other terms, the outgoing active power does not exceed the incoming active power.

3.1 Generalized Lossless Scattering

A scattering junction is said to be *lossless* if $\mathcal{P}^+ = \mathcal{P}^-$, i.e., the active power absorbed at the junction is zero. In the case of lossless propagation in a passive medium, it is easy to verify from (19), (23) and (24) that this is ensured if and only if

$$\boldsymbol{\Gamma}(z) = \boldsymbol{A}^*\boldsymbol{\Gamma}(z)\boldsymbol{A} \tag{26}$$

where $\boldsymbol{\Gamma}(z)$ is a generalized wave admittance which is para-Hermitian and analytic for $|z| > 1$[6]. In this case the matrix $\boldsymbol{A}$ is said to be a *lossless scattering matrix*. We refer to (26) as the *condition of losslessness*.

When wave propagation occurs in a medium which is passive but not necessarily lossless, the condition for lossless scattering becomes

$$\boldsymbol{\Gamma}^*(1/z^*) = \boldsymbol{A}^*\boldsymbol{\Gamma}(z)\boldsymbol{A} \tag{27}$$

Notice that (26) is closely related to the well-known

[6]Note that by the maximum modulus theorem, if a matrix of meromorphic functions is positive definite on the unit circle and analytic outside the unit circle, it is necessarily positive definite everywhere outside the unit circle.

Lyapunov equation [43] for testing the asymptotic stability of discrete-time linear systems.

The definition of lossless junctions employed here includes junctions arising from the connection of physical waveguides, and extends the formal treatment to non-physical junctions as well. In certain applications, it can be useful to use non-physical scattering matrices having a particular structure which increases the computational efficiency, or which gives the desired behavior of the system [78, 79].

In DWNs, waveguide sections separating scattering junctions are normally implemented using delay lines. Since in any physical simulation there will be delay in both directions, the delay lines isolate the scattering junctions, allowing parallel computation of the junctions. This is an advantage over traditional ladder/lattice filters in which delay elements are present in only one flow direction [57, 92], thus preventing both a direct pipelined computation and a physical interpretation. On the other hand, having the delays along only one direction is easier to work with when the problem is to realize a ladder/lattice filter having a prescribed transfer function [57, 112].

4 The Normalized Lossless Junction

In some applications it is worthwhile to *normalize* the traveling waves so that all waveguides effectively have unit impedance, $\boldsymbol{R}(z) = \boldsymbol{I}$. To normalize, pressure waves are multiplied by a (matrix) square root of the wave admittance, and velocity waves are multiplied by a (matrix) square root of the wave impedance. Conservation of power at a lossless junction implies that the signal dynamic range is conserved in a mean square sense for normalized waves. This can be very useful in fixed-point implementations of large networks, especially in the time-varying case, since signal scaling problems are avoided and the full dynamic range can be achieved at every point of the network. Normalized waveguide networks can be seen as a generalization of the normalized ladder filter [35].

4.1 Time-Varying Normalized Waveguide Networks

A *time-varying* waveguide network can be created by changing one or more impedances over time. This induces changes in the scattering junctions connecting the various impedances. Defining time variation this way also preserves the physical interpretation of the time-varying network which is critical for keeping a handle on passivity and hence on stability and numerical robustness.

Since the signal power associated with, say, a single traveling pressure sample $p(n)$ stored within a delay element in a scalar digital waveguide is $\mathcal{P}_{p(n)} = p^2(n)\Gamma$, where Γ is the (scalar) wave admittance of the associated waveguide, modulating a waveguide impedance also modulates the stored signal power in that waveguide. That is, the stored power associated with the sample $p(n)$ varies proportional to $\Gamma(n)$. This is not the case with normalized waves. The normalized counterpart of pressure sample $p(n)$ is $\tilde{p}(n) = p(n)\sqrt{\Gamma(n)}$, and the associated power is always just the square of the sample value: $\mathcal{P}_{\tilde{p}(n)} = \tilde{p}^2(n) = p^2(n)\Gamma(n) = \mathcal{P}_{p(n)}$. The scattering junctions connecting normalized waveguides are modulated by the time-varying impedances, but the stored signal power in the normalized waveguides is not. For the case of lossless scattering junctions, signal energy is constant throughout the time-varying network. This gives a general class of energy conserving time-varying digital filters which, along with passive rounding rules, are also free of limit cycles and overflow oscillations [92]. Thus, normalized waveguide networks decouple signal power in the network from time variations in the scattering coefficients: A change in the wave impedance

changes the scattering properties of the junctions but does not alter the instantaneous signal power in the network.

4.2 Isolating Time-Varying Junctions

Since waveguide sections are typically terminated on both ends by scattering junctions, a change in one waveguide impedance modulates both scattering junctions rather than only one as may be desired. It is possible to vary the coefficients of only a single junction when the network is an acyclic graph (which can be thought of as a generalization of the cascade chain as used in ladder/lattice filters). Consider the simple case of the cascade chain: Suppose there are N waveguides abutted end to end and numbered 1 through N from left to right. Suppose further that we want to modulate only the scattering junction between sections m and $m+1$. We can accomplish this by modulating the impedance R_{m+1} of section $m+1$. Let the modulation signal be denoted by $g(n) = R_{m+1}(n)/R_{m+1}(0)$, assuming the modulation begins after time 0. Then we can cancel the modulation at the right endpoint of section $m+1$ by modulating the impedance of section $m+2$ by $g(n)$ (since the scattering coefficients at the junction of two waveguides depends only on the impedance ratio). However, now we have to also modulate the impedance of section $m+3$ by $g(n)$ in order to prevent modulation at the junction of sections $m+2$ and $m+3$. Continuing in this way, we must modulate the impedances of all waveguides to the right of section m by $g(n)$ in order to obtain an isolated modulated junction between sections m and $m+1$. This argument extends readily to an acyclic graph, and breaks down whenever a "downstream" branch is connected to an "upstream" branch, i.e., whenever there is a cycle in the waveguide network graph.

The simultaneous variation of many wave impedances determines an instantaneous variation of the stored signal power. When the waveguides are normalized, the signal power remains fixed. As a result, it is possible to vary isolated junctions in the normalized case without worrying about energy modulation consequences in other parts of the network.

Another way to isolate impedance variations in a time-varying network is by means of ideal *transformers* which can step the wave impedance up or down by an arbitrary factor without inducing reflections. The basic theory of the digital waveguide transformer is discussed in Appendix A, and Section 9 discusses further applications.

4.3 Scattering of Normalized Waves

We consider first *diagonal* impedance matrices, since they have an intuitive physical counterpart in lossless acoustic tubes. Under this assumption, we have the impedance matrix

$$\boldsymbol{R} = \mathrm{diag}[R_1, \ldots, R_n] \tag{28}$$

and the admittance matrix

$$\boldsymbol{\Gamma} = \mathrm{diag}[\Gamma_1, \ldots, \Gamma_n] = \boldsymbol{R}^{-1}. \tag{29}$$

By (19) and the assumption of a passive medium, the normalized pressure waves are uniquely defined as

$$\tilde{p}_i^{\pm} = \frac{p_i^{\pm}}{\sqrt{R_i}} = p_i^{\pm}\sqrt{\Gamma_i} \tag{30}$$

where the three signs above are all taken as "+" or all as "−". (Square roots in this paper are always taken as positive.) We can write also

$$\tilde{\boldsymbol{p}}^{\pm} = \boldsymbol{\Gamma}^{\frac{1}{2}}\boldsymbol{p}^{\pm} \tag{31}$$

where $\mathbf{\Gamma}^{\frac{1}{2}}$ is the diagonal square root of $\mathbf{\Gamma}$. The junction of normalized waveguides is in this case represented by the scattering matrix

$$\tilde{\boldsymbol{A}} = \mathbf{\Gamma}^{\frac{1}{2}} \boldsymbol{A} \mathbf{\Gamma}^{-\frac{1}{2}} \tag{32}$$

As a side note, this equation is analogous to the relation between power-wave scattering matrices and voltage-wave scattering matrices as found in the WDF literature [27] for lumped circuit elements.

In the more general case, when the (complex) admittance matrix Γ is not necessarily diagonal, but remains positive semidefinite as required for lossless propagation, we have that $\mathbf{\Gamma}$ admits a Cholesky factorization

$$\mathbf{\Gamma} = \boldsymbol{U}^* \boldsymbol{U} \tag{33}$$

where $\boldsymbol{U}$ is upper triangular. We can define the normalized pressure waves as

$$\tilde{\boldsymbol{p}}^{\pm} = \boldsymbol{U} \boldsymbol{p}^{\pm} \tag{34}$$

The normalized scattering junction is obtained via the following similarity transformation on the unnormalized scattering matrix:

$$\tilde{\boldsymbol{A}} = \boldsymbol{U} \boldsymbol{A} \boldsymbol{U}^{-1} \tag{35}$$

Theorem 1 *The scattering matrix of a normalized junction is* unitary*, i.e.,*

$$\tilde{\boldsymbol{A}}^* \tilde{\boldsymbol{A}} = \boldsymbol{I} \tag{36}$$

Proof: From the condition of losslessness (26), we have $\tilde{\boldsymbol{A}}^* \tilde{\boldsymbol{A}} = \boldsymbol{U}^{-*} \boldsymbol{A}^* \boldsymbol{U}^* \boldsymbol{U} \boldsymbol{A} \boldsymbol{U}^{-1} = \boldsymbol{U}^{-*} \boldsymbol{A}^* \mathbf{\Gamma} \boldsymbol{A} \boldsymbol{U}^{-1} = \boldsymbol{U}^{-*} \mathbf{\Gamma} \boldsymbol{U}^{-1} = \boldsymbol{U}^{-*} \boldsymbol{U}^* \boldsymbol{U} \boldsymbol{U}^{-1} = \boldsymbol{I}$

By an explicit computation of the matrix product in (36) we can show that the terms of any column of $\tilde{\boldsymbol{A}}$ are *power complementary*, i.e.,

$$\sum_{i=1}^{N} | \, \tilde{a}_{i,k} \, |^2 = 1 \tag{37}$$

for all k.

5 Physical Scattering Junctions

All scattering matrices arising from the connection of N scalar physical waveguides have the same basic structure which is an efficient subset of the set of all lossless scattering matrices in the sense of (26). To fix the setting, consider the parallel junction of N lossless acoustic tubes, each with real, positive, scalar wave admittance Γ_i. The pressure at the junction is the same for all N waveguides at the junction point, and the velocities from each branch sum to zero. These physical constraints yield scattering matrices of the form

$$\begin{aligned} \boldsymbol{A} &= \begin{bmatrix} \frac{2\Gamma_1}{\Gamma_J} - 1 & \frac{2\Gamma_2}{\Gamma_J} & \cdots & \frac{2\Gamma_N}{\Gamma_J} \\ \frac{2\Gamma_1}{\Gamma_J} & \frac{2\Gamma_2}{\Gamma_J} - 1 & \cdots & \frac{2\Gamma_N}{\Gamma_J} \\ \cdots & & & \\ \frac{2\Gamma_1}{\Gamma_J} & \frac{2\Gamma_2}{\Gamma_J} & \cdots & \frac{2\Gamma_N}{\Gamma_J} - 1 \end{bmatrix} \\ &\triangleq \mathbf{1} \boldsymbol{\alpha}^T - \boldsymbol{I} \end{aligned} \tag{38}$$

where Γ_J and $\boldsymbol{\alpha}$ are defined as follows:

$$\Gamma_J = \sum_{i=1}^{N} \Gamma_i \tag{39}$$

$$\boldsymbol{\alpha} \stackrel{\triangle}{=} \frac{2}{\Gamma_J}[\Gamma_1, \ldots, \Gamma_N]^T \tag{40}$$

It is easy to verify that the matrix $\boldsymbol{A}$ satisfies the condition of losslessness (26). In the particular case of equal-impedance waveguides, we have

$$\begin{aligned} \boldsymbol{A}_e &= \begin{bmatrix} \frac{2}{N}-1 & \frac{2}{N} & \ldots & \frac{2}{N} \\ \frac{2}{N} & \frac{2}{N}-1 & \ldots & \frac{2}{N} \\ \ldots & & & \\ \frac{2}{N} & \frac{2}{N} & \ldots & \frac{2}{N}-1 \end{bmatrix} \\ &\stackrel{\triangle}{=} \frac{2}{N}\mathbf{1}\mathbf{1}^T - \boldsymbol{I} \end{aligned} \tag{41}$$

We notice that the elements of each row of matrix $\boldsymbol{A}$ in (38) and (41) are *allpass complementary*, i.e., $|\sum_{k=1}^{N} a_{i,k}| = 1$, for all k. Since the scattering matrix $\boldsymbol{A}_e$ for equal-impedance waveguides is symmetric, the elements of any row or column of matrix $\boldsymbol{A}_e$ are allpass complementary. Since $\boldsymbol{A}_e$ remains unchanged in the normalized case, the elements of each row and column are also power complementary.

The equal-impedance case is particularly important when N is a power of two. In this case, all the multiplications can be replaced by right-shifts in fixed-point arithmetic, and considerable savings in circuit area can be achieved in a VLSI implementation. This case has been explored in the design of efficient digital waveguide meshes [91, 122, 125].

The scattering matrix for a connection of N normalized physical waveguides is given by (32). It can be more explicitly written as

$$\begin{aligned} \tilde{\boldsymbol{A}} &= \begin{bmatrix} \frac{2\Gamma_1}{\Gamma_J}-1 & \frac{2\sqrt{\Gamma_1\Gamma_2}}{\Gamma_J} & \ldots & \frac{2\sqrt{\Gamma_1\Gamma_N}}{\Gamma_J} \\ \frac{2\sqrt{\Gamma_2\Gamma_1}}{\Gamma_J} & \frac{2\Gamma_2}{\Gamma_J}-1 & \ldots & \frac{2\sqrt{\Gamma_2\Gamma_N}}{\Gamma_J} \\ \ldots & & \ldots & \\ \ldots & & \ldots & \\ \frac{2\sqrt{\Gamma_N\Gamma_1}}{\Gamma_J} & \frac{2\sqrt{\Gamma_N\Gamma_2}}{\Gamma_J} & \ldots & \frac{2\Gamma_N}{\Gamma_J}-1 \end{bmatrix} \\ &\stackrel{\triangle}{=} 2\boldsymbol{\gamma}\boldsymbol{\gamma}^T - \boldsymbol{I} \end{aligned} \tag{42}$$

where $\boldsymbol{\gamma} \stackrel{\triangle}{=} \frac{2}{\sqrt{\Gamma_J}}[\sqrt{\Gamma}_1, \ldots, \sqrt{\Gamma}_N]^T$, and the power-complementary property (37) can be verified for both rows and columns.

In the expressions (38)–(42), the elements of the matrices are real, since the one-variable waveguides intersecting at the junction have real, positive impedances.

Normalized N-way scattering junctions represented by real matrices can be implemented by $N(N-1)/2$ CORDIC processors [38]. Since the scattering matrix is orthogonal (real and unitary), it corresponds to a rotation in N dimensions. Any such rotation can be obtained by $N(N-1)/2$

planar rotations [34], with each planar rotation being realizable using a CORDIC processor. This formulation can be useful for VLSI implementations.

The junction represented by the expressions (38) to (42) is formally a *parallel* junction. The corresponding *series* junction can be obtained by taking the *dual* of the parallel junction, i.e., by replacing admittance with impedance and interchanging pressure and velocity. In the series junction, the velocity is the same in all waveguides at the junction, and the pressures (or forces) sum to zero.

Parallel junctions occur naturally in the case of intersecting acoustic tubes, while series junctions arise at the intersection of N transversely vibrating strings, where the transverse velocity must be the same for all N strings. For waves in strings, force waves play the role of pressure waves in acoustic tubes. Note that the wave equation (1) for strings is usually written in terms of transverse displacement. However, choosing velocity and force as Kirchhoff variables unifies the treatment of vibrating strings with that of acoustic tubes.

5.1 Parallel Junction of Multivariable Complex Waveguides

We now consider the scattering matrix for the parallel junction of N m-variable physical waveguides, and at the same time, we treat the generalized case of matrix transfer-function wave impedances. Equations (13) and (11) can be rewritten for each m-variable branch as

$$\begin{array}{rcrcl} \boldsymbol{u}_i^+ & = & & \boldsymbol{\Gamma}_i(z) & \boldsymbol{p}_i^+ \\ \boldsymbol{u}_i^- & = & - & \boldsymbol{\Gamma}_i^*(1/z^*) & \boldsymbol{p}_i^- \end{array} \tag{43}$$

and

$$\begin{array}{l} \boldsymbol{u}_i = \boldsymbol{u}_i^+ + \boldsymbol{u}_i^- \\ \boldsymbol{p}_i = \boldsymbol{p}_i^+ + \boldsymbol{p}_i^- = p_J \mathbf{1} \end{array} \tag{44}$$

where $\boldsymbol{\Gamma}_i(z) = \boldsymbol{R}_i^{-1}(z)$, p_J is the pressure at the junction, and we have used pressure continuity to equate $\boldsymbol{p}_i$ to p_J for any i.

Using conservation of velocity we obtain

$$\begin{aligned} 0 &= \mathbf{1}^T \sum_{i=1}^{N} \boldsymbol{u}_i \\ &= \mathbf{1}^T \sum_{i=1}^{N} \Big\{ \left[\boldsymbol{\Gamma}_i(z) + \boldsymbol{\Gamma}_i^*(1/z^*)\right] \boldsymbol{p}_i^+ \\ &\qquad -\boldsymbol{\Gamma}_i^*(1/z^*) p_J \mathbf{1} \Big\} \end{aligned} \tag{45}$$

and

$$p_J = S \mathbf{1}^T \sum_{i=1}^{N} \left[\boldsymbol{\Gamma}_i(z) + \boldsymbol{\Gamma}_i^*(1/z^*)\right] \boldsymbol{p}_i^+ \tag{46}$$

where

$$S = \left\{ \mathbf{1}^T \left[\sum_{i=1}^{N} \boldsymbol{\Gamma}_i^*(1/z^*) \right] \mathbf{1} \right\}^{-1}. \tag{47}$$

Hence, the scattering matrix is given by

$$\boldsymbol{A} = S \left[\begin{array}{c} \mathbf{1}^T \left[\begin{array}{ccc} \boldsymbol{\Gamma}_1 + \boldsymbol{\Gamma}_1^* & \ldots & \boldsymbol{\Gamma}_N + \boldsymbol{\Gamma}_N^* \end{array} \right] \\ \ldots \\ \mathbf{1}^T \left[\begin{array}{ccc} \boldsymbol{\Gamma}_1 + \boldsymbol{\Gamma}_1^* & \ldots & \boldsymbol{\Gamma}_N + \boldsymbol{\Gamma}_N^* \end{array} \right] \end{array} \right] - \boldsymbol{I} \tag{48}$$

It is clear that (38) is a special case of (48) when $m = 1$. If the branches do not all have the same dimensionality m, we may still use the expression (48) by letting m be the largest dimensionality and embedding each branch in an m-variable propagation space.

5.2 Loaded Junctions

In discrete-time modeling of acoustic systems, it is often useful to attach waveguide junctions to external dynamic systems which act as a *load*. We speak in this case of a *loaded junction*. The load is expressed in general by its complex admittance and can be considered a lumped circuit attached to the distributed waveguide network.

Examples of loaded junctions can be found in certain representations of finger holes in wind-instrument modeling [93, 80], or in bridge terminations in stringed-instrument modeling [98] (see the example in the next section). They are also a natural way to load a waveguide mesh to simulate air above a membrane [31]. Sometimes the load can be time-varying and even nonlinear, as in the case of a piano hammer hitting a string [127, 7]; in this case, the hammer is modeled as a mass-spring system in which the spring stiffness nonlinearly depends on its compression, and the impedance "seen" by the string changes continuously during contact. Finally, the loaded junction equations can be used to interface a DWN with other types of physical modeling simulations (e.g., a WDF): In such a case, the attached load is simply the driving-point impedance of the external simulation.

To derive the scattering matrix for the *loaded* parallel junction of N lossless acoustic tubes, the Kirchhoff's node equation is reformulated so that the sum of velocities meeting at the junction equals the exit velocity (instead of zero). For the series junction of transversely vibrating strings, the sum of forces exerted by the strings on the junction is set equal to the force acting on the load (instead of zero).

The load admittance Γ_L is regarded as a *lumped driving-point admittance* [128], and the equation

$$U_L(z) = \Gamma_L(z) p_J(z) \tag{49}$$

expresses the relation at the load. In acoustic modeling applications, Γ_L is normally first obtained in the continuous-time case as a function of the Laplace transform variable s. Denote the continuous-time Laplace transform by $\Gamma_L^c(s)$, and the inverse Laplace transform by $\gamma_L^c(t)$. To preserve the tuning of audio resonances of acoustic systems, the load admittance is usually converted to discrete time by the impulse-invariant method, i.e., simple sampling of $\gamma_L^c(t)$ in the time domain. In simpler cases in which there is only one resonance to be transformed from the s plane to the z plane, such as a piano-hammer model (a mass-spring system) or the individual terms of a partial fraction expansion, the bilinear transform $s = \alpha(z-1)/(z+1)$ may be used [65].

In the impulse-invariant case, to avoid aliasing, we require $\Gamma_L^c \simeq 0$ for frequencies near and above half the sampling rate. Since the driving-point admittances of acoustic systems are not generally bandlimited (consider the driving-point impedance of an elementary mass $\Gamma_L^c(s) = 1/ms$ or spring $\Gamma_L^c(s) = Ks$), anti-aliasing filtering should be applied to $\gamma_L^c(t)$. The bilinear transform is

inherently free of aliasing since the entire $j\omega$ axis in the s plane is mapped only once to the unit circle in the z plane, but as a result of this mapping, the frequency axis is *warped*, and the behavior at continuous-time frequencies can be mapped to the same discrete-time frequencies at only three points (dc, half the sampling rate, and one more frequency which is arbitrary). For this reason, the impulse-invariant method is normally preferred when the precise tuning of more than one spectral feature is important.

In case of a time-varying or nonlinear load, as in the piano-hammer model, to avoid aliasing, the load impedance should vary sufficiently slowly and/or be sufficiently weakly nonlinear so that the low-pass filtering in the DWN will attenuate modulation and/or distortion products to insignificance before aliasing occurs in the recursive network.

The scattering matrix for a *loaded* parallel junction of N lossless, scalar waveguides with real wave impedances can be rewritten as [93]

$$\boldsymbol{A}_L = \begin{bmatrix} \frac{2\Gamma_1}{\Gamma_J} - 1 & \frac{2\Gamma_2}{\Gamma_J} & \cdots & \frac{2\Gamma_N}{\Gamma_J} \\ \\ \frac{2\Gamma_1}{\Gamma_J} & \frac{2\Gamma_2}{\Gamma_J} - 1 & \cdots & \frac{2\Gamma_N}{\Gamma_J} \\ \cdots & & \cdots & \\ \cdots & & \cdots & \\ \frac{2\Gamma_1}{\Gamma_J} & \frac{2\Gamma_2}{\Gamma_J} & \cdots & \frac{2\Gamma_N}{\Gamma_J} - 1 \end{bmatrix}$$

where

$$\Gamma_J = \Gamma_L + \sum_{i=1}^{N} \Gamma_i \tag{50}$$

For the more general case of N m-variable physical waveguides, the expression of the scattering matrix is that of (48), with

$$S = \left[\mathbf{1}^T \left(\sum_{i=1}^{N} \boldsymbol{\Gamma}_i \right) \mathbf{1} + \Gamma_L \right]^{-1} \tag{51}$$

5.3 Example: Bridge Coupling of Piano Strings

As an application of the theory, we outline the digital simulation of two pairs of piano strings. The strings are attached to a common bridge which acts as a coupling element between the strings (see Fig. 3). An in-depth treatment of coupled strings can be found in [132].

To a first approximation, the bridge can be modeled as a lumped mass-spring-damper system, while for the strings, a distributed waveguide representation is more appropriate. For the purpose of illustrating the theory in its general form, we represent each pair of strings as a single 2-variable waveguide. This approach is justified if we associate the pair with the same key in such a way that both the strings are subject to the same excitation. Since the 2×2 matrices $\boldsymbol{M}$ and $\boldsymbol{T}$ of (5) can be considered to be diagonal in this case, we could alternatively describe the system as four separate scalar waveguides.

The i^{th} pair of strings is described by the 2-variable impedance matrix

$$\boldsymbol{R}_i = \begin{bmatrix} R_{i,1} & 0 \\ 0 & R_{i,2} \end{bmatrix} \tag{52}$$

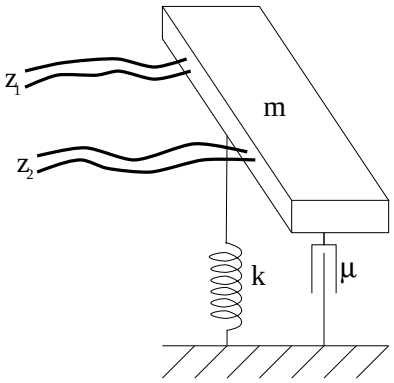

Figure 3: Two pairs of strings coupled at a bridge.

The lumped elements forming the bridge are connected in series, so that the driving-point velocity[7] u is the same for the spring, mass, and damper:

$$u(t) = u_m(t) = u_k(t) = u_\mu(t) \tag{53}$$

Also, the forces provided by the spring, mass, and damper, sum:

$$p(t) = p_m(t) + p_k(t) + p_\mu(t) \tag{54}$$

We can derive an expression for the bridge impedances using the following relations in the Laplace-transform domain:

$$\begin{aligned} P_k(s) &= (k/s)U_k(s) \\ P_m(s) &= msU_m(s) \\ P_\mu(s) &= \mu U_\mu(s) \end{aligned} \tag{55}$$

Equations (55) and (54) give the continuous-time load impedance

$$R_L(s) = \frac{P(s)}{U(s)} = m\frac{s^2 + s\mu/m + k/m}{s} \tag{56}$$

In order to move to the discrete-time domain, we may apply the bilinear transform

$$s \leftarrow \alpha\frac{1 - z^{-1}}{1 + z^{-1}} \tag{57}$$

to (56). The factor α is used to control the compression of the frequency axis. It may be set to $2/T$ so that the discrete-time filter corresponds to integrating the analog differential equation using the trapezoidal method, or it may be chosen to preserve the resonance frequency (preferred).

We obtain

$$\begin{aligned} R_L(z) &= \Big[(\alpha^2 - \alpha\mu/m + k/m)z^{-2} \\ &+ (-2\alpha^2 + 2k/m)z^{-1} \\ &+ (\alpha^2 + \alpha\mu/m + k/m)\Big] \Big/ \Big[\alpha/m(1 - z^{-2})\Big] \end{aligned}$$

[7]The symbols for the variables velocity and force have been chosen to maintain consistency with the analogous acoustical quantities.

The factor S in the impedance formulation of the scattering matrix (48) is given by

$$S(z) = \left[\sum_{i,j=1}^{2} R_{i,j} + R_L(z)\right]^{-1} \tag{58}$$

which is a rational function of the complex variable z. The scattering matrix is given by

$$\boldsymbol{A} = 2S \begin{bmatrix} R_{1,1} & R_{1,2} & R_{2,1} & R_{2,2} \\ R_{1,1} & R_{1,2} & R_{2,1} & R_{2,2} \\ R_{1,1} & R_{1,2} & R_{2,1} & R_{2,2} \\ R_{1,1} & R_{1,2} & R_{2,1} & R_{2,2} \end{bmatrix} - \boldsymbol{I} \tag{59}$$

which can be implemented using a *single* second-order filter having transfer function (58).

6 Nonlinear, Time-Varying DWNs

The DWN paradigm is highly useful for constructing time-varying nonlinear digital filters which are guaranteed *stable* in the Lyapunov sense [59, 25]. Lyapunov stability analysis involves finding a positive-definite "Lyapunov function" (which is like a norm defined on the filter state), which decreases each time step (given zero inputs) in the presence of linear or nonlinear computations (such as numerical round-off). Whenever each state variable (delay element) in a filter computation has a physical interpretation as an independent wave variable, a Lyapunov function can be defined simply as the sum of wave energies associated with the state variables. By choosing the scattering-junction round-off rules to be passive (e.g., by using magnitude truncation), the total stored energy in the filter decreases or remains the same relative to an infinite-precision implementation. As long as the infinite-precision filter is asymptotically stable, the quantized filter must be also. Thus, the total stored energy in any "physical" digital filter is precisely what is needed for a Lyapunov function.

Since many ladder, lattice, and wave digital filters are equivalent to DWNs, possibly after some delay manipulations [51, 92, 93, 75], it is clear that DWNs can be used to realize a wide class of transfer functions. In particular, every filter transfer function can be realized as a linear combination of DWNs (in a manner analogous to using "tap parameters" on a ladder or lattice filter [57, 12]), and linear combinations are well behaved in the presence of nonlinearities and time-varying parameters.

In practice, Lyapunov stability in a DWN is normally guaranteed by ensuring that wave-variables are never *amplified* by nonlinear operations or time-varying gains. For example, magnitude truncation on each output of an extended-precision scattering junction suffices to ensure passivity. Non-amplifying nonlinearities and varying gains are sufficient for passivity but sometimes too dissipative, especially in waveguide mesh applications [122]. A more refined rule is obtained by summing rounded-off energy (or an approximation to it) in an accumulator and changing the direction of rounding so as to servo the cumulative energy error to zero [93].

In the normalized case, the energy associated with each signal sample in a DWN is given by the square of that sample,[8] so the total energy stored in a DWN is given simply as the sum of

[8]Strictly speaking, a squared wave variable in a normalized waveguide is proportional to signal *power* [97], and we should multiply by the sampling interval T to obtain units of energy. However, such a constant scale factor is inconsequential.

squares of all the samples contained in all the delay elements. In the unnormalized case, the energy of the jth sample $x_{i,j}(n)$ in waveguide i, at time n, is given by $x_{i,j}^2(n)/R_i$, where R_i is the wave impedance of the ith waveguide, and the total energy at time n in the DWN can be written as

$$\mathcal{E}(n) = \sum_{i=1}^{N} \sum_{j=1}^{M_i} \frac{x_{i,j}^2(n)}{R_i}.$$

where M_i is the length of waveguide i in samples. The DWN is stable in the presence of time-varying nonlinearities so long as $\mathcal{E}(n)$ (the Lyapunov functional for the DWN) is not increased when all inputs are zero, i.e.,

$$\mathcal{E}(n+1) \leq \mathcal{E}(n).$$

Thus, *magnitude truncation* (rounding toward zero) at the output of all scattering junctions (with extended precision internal to each junction) preserves network stability, as does multiplication of any wave variable by a nonlinear or time-varying gain $g_{i,j}(n)$ not exceeding 1 in magnitude, i.e., we only require $|g_{i,j}(n)| \leq 1$, for all n.

The above general result is applied in the following specific example (which is related to a waveguide sitar model):

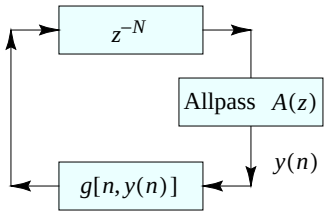

Figure 4: A feedback loop containing a delay line, an allpass filter, and a time-varying nonlinearity.

Theorem 2 *A feedback loop containing an allpass filter $A(z)$ (assumed here to be exactly implemented), a delay line of any length $N > 0$, and a time-varying nonlinearity $g[n, y(n)]$, as shown in Fig. 4, is stable in the Lyapunov sense if $|g[n, y(n)]| \leq 1$ for all n. If the initial stored energy is $\mathcal{E}(0)$, then the total energy remaining at time n is given by*

$$\mathcal{E}(n) = \mathcal{E}(0) - \sum_{i=1}^{n} \{1 - g^2[i, y(i)]\} y^2(i)$$

Proof: It suffices to show that (a) the arrangement of Fig. 4 is numerically equivalent to a DWN, and (b) $y(n)$ is a wave variable of the DWN corresponding to a unit impedance. Consider the redrawing of Fig. 4 as in Fig. 5. The delay line is broken into two halves to form a digital waveguide. (If the delay line length is odd, a sample of delay can be moved in cascade with the allpass filter.) It is well known that an arbitrary order M allpass filter can be realized in the form of a digital ladder filter [57] with no "taps," and it is straightforward to show that such a ladder filter can be manipulated into a digital waveguide filter by splitting each unit delay into two half-delays and commuting half of the half-delays around the ladder so that there is a half-delay between each

scattering junction on both the upper and lower rails of the lattice [92].[9] In this configuration, also shown in Fig. 5, the ladder filter is a DWN consisting of a cascade of digital waveguides, where the input and output of the allpass are the incoming and outgoing wave variables at the left of the leftmost waveguide of the allpass, and the rightmost waveguide is terminated on the right by a perfect reflection (infinite wave impedance, given pressure or force waves). Without loss of generality, we may choose the wave impedance of the bidirectional delay line to be 1. The return signal $y(n)$ from the allpass is a wave variable at wave impedance 1, and its energy at time n is $y^2(n)$. After scaling by the nonlinearity, its energy becomes $|g[n, y(n)]|^2 y^2(n)$, and the energy lost each sample interval is therefore $\{1 - g^2[n, y(n)]\}y^2(n)$, which is nonnegative, and the total energy lost is simply the sum over time of these per-sample losses.

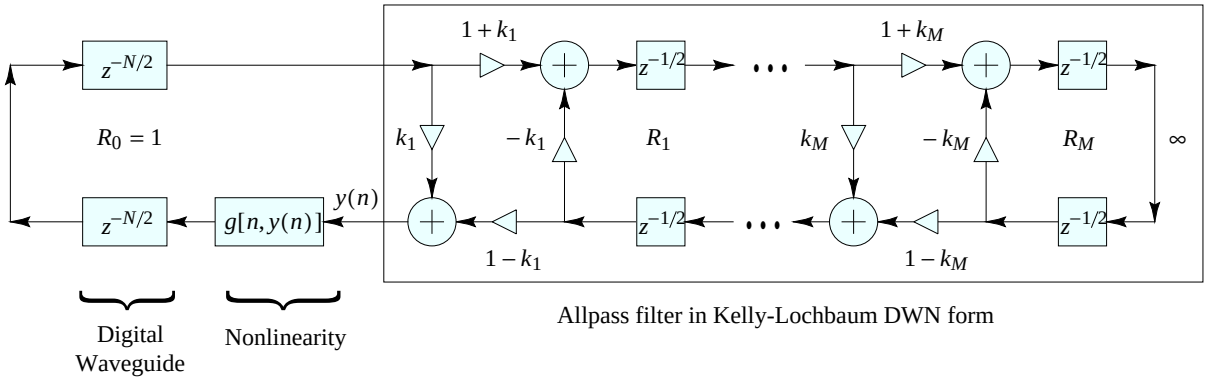

Figure 5: A system equivalent to Fig. 4 containing a bidirectional delay line (digital waveguide) terminated reflectively on the left, terminated on the right by an allpass reflectance, and containing a time-varying nonlinearity on the return wave from the allpass.

Corollary 1 *All* lossless *nonlinearities or time-varying gains in the system of Fig. 4 can only select between the values* $+1$ *and* -1.

Corollary 2 *The amplitude of* $y(n)$ *is bounded by* $y(n) \leq \sqrt{\mathcal{E}(n)}$.

Corollary 3 *The signal* $y(n)$ *will approach zero asymptotically so long as* $|g[n, y(n)]| \leq 1 - \epsilon$ *for some fixed* $\epsilon > 0$, *irrespective of how* g *may vary with time or as a function of* y.

Of course, by keeping track of the energy gained or lost, as illustrated in the above theorem, and by controlling the gain/nonlinearity so that energy gained or lost is compensated at a later time, a wider class of nonlinear and/or time-varying systems may be defined which are lossless *on average*. An example is the exactly lossless (on average) DWN which servos round-off error energy to zero mentioned above. It is also possible to approximate lossless nonlinear behavior within the allpass filter [67, 127].

[9] Altering a ladder filter to convert it to a DWN can also be accomplished using the cut-set method of Kung [51, 12].

7 Algebraic Properties of Lossless Junctions

Comparing (38) and (42) shows that the elements of the normalized scattering matrix $\tilde{\boldsymbol{A}}$ in (42) are

$$\tilde{a}_{i,j} = a_{i,j}\frac{\sqrt{\Gamma_i}}{\sqrt{\Gamma_j}} = 2\sqrt{\Gamma_i\Gamma_j}\Big/\sum_{k=1}^{N}\Gamma_k - \delta(i-j) = \tilde{a}_{j,i} \tag{60}$$

where $\delta(n)\stackrel{\triangle}{=}1$ for $n=0$ and 0 for $n\neq 0$. Hence, the normalized scattering matrix $\tilde{\boldsymbol{A}}$ is symmetric. As was shown in Theorem 1, it is easy to verify by direct computation that $\tilde{\boldsymbol{A}}$ is also unitary (i.e., $\tilde{\boldsymbol{A}}\tilde{\boldsymbol{A}}^* = \tilde{\boldsymbol{A}}^*\tilde{\boldsymbol{A}} = \boldsymbol{I}$), so that all its eigenvalues are on the unit circle. Since all eigenvalues of a real, symmetric matrix are real [66], $\tilde{\boldsymbol{A}}$ has eigenvalues only at ± 1. Moreover, since by (32) $\tilde{\boldsymbol{A}}$ and $\boldsymbol{A}$ are related by a similarity transformation, $\boldsymbol{A}$ also must have all eigenvalues at $+1$ or -1.

An elementary eigenvector analysis can be conducted using physical analogies. It is well known that a symmetric matrix has orthogonal eigenvectors. For the equal-impedance case, one eigenvector is always $e_0 = \left[\begin{array}{cccc} 1 & 1 & \ldots & 1 \end{array}\right]^T$ by symmetry: this corresponds to a collision of equal pressure waves at the junction, so the return scatter must be identical. This corresponds to the eigenvalue 1. For the -1 eigenvalues, a similar interpretation can be found: inject a unit pressure wave at all the branches but one, and "pull out" a pressure wave having magnitude $N-1$ at the remaining branch. In this case, the return scatter is inverted, since we have arranged that the pressure be zero at the junction and hence at each branch termination. In this way we can find N eigenvectors analogous with $e_1 = \left[\begin{array}{cccc} -(N-1) & 1 & \ldots & 1 \end{array}\right]^T$ which span the $(N-1)$-dimensional subspace associated with the eigenvalue -1. Note that e_0 is orthogonal to this subspace, while the e_i are not mutually orthogonal for $i>0$.

For unequal impedances, a similar physical interpretation can be found for the eigenvectors. If we supply equal pressure waves to all branches at the junction, the reflected waves must be equal by symmetry, since $p_i^- = p_J - p_i^+$, where p_J is the junction pressure and all the p_i^+ are equal. Hence, $e_0 = \left[\begin{array}{cccc} 1 & 1 & \ldots & 1 \end{array}\right]^T$ remains an eigenvector corresponding to the eigenvalue 1. On the other hand, if we inject a unit pressure wave into all the branches but the jth and "pull out" a pressure wave having magnitude $\sum_{i\neq j}\Gamma_i/\Gamma_j$ at the jth branch, then the junction pressure p_J is again forced to zero by construction and the return scatter at any branch is the negative of the incoming wave on that branch. In this way we can find N eigenvectors analogous with $e_j = \left[\begin{array}{ccccccc} 1 & \ldots & 1 & -\sum_{i\neq j}\Gamma_i/\Gamma_j & 1 & \ldots & 1 \end{array}\right]^T$ spanning the $(N-1)$-dimensional subspace associated with the eigenvalue -1. In this case, none of the eigenvectors is necessarily orthogonal to the others.

The foregoing is an example of how physical intuition can help in finding algebraic properties of a given matrix in physical applications.

Another property of the scattering matrix $\boldsymbol{A}$ is that it is its own inverse: $\boldsymbol{A}^2 = \boldsymbol{I}$. This corresponds physically to the fact that if the results of a scattering operation are fed back to the same junction as incoming waves, the result must be the inverse of the original scattering. An implication of this is that lossless scattering networks can be run in *reverse,* i.e., by changing the directions of all the delay lines and computing the junctions as dictated by the wave impedances, the network will compute its own inverse. If there are inputs and outputs, they must be interchanged.

7.1 Conditions for Lossless Scattering

We now present a theorem characterizing the condition of losslessness in terms of the eigenvalues and eigenvectors of the scattering matrix.

Theorem 3 *A scattering matrix $\boldsymbol{A} \in \mathcal{C}^{N\times N}$ is lossless if and only if its eigenvalues lie on the unit circle and it admits a basis of N linearly independent eigenvectors.*

Proof: By definition (26), $\boldsymbol{A}$ is lossless if $\boldsymbol{A}^*\boldsymbol{\Gamma}\boldsymbol{A} = \boldsymbol{\Gamma}$, where $\boldsymbol{\Gamma}$ is a positive definite matrix. Therefore, $\boldsymbol{\Gamma}$ admits a Cholesky factorization $\boldsymbol{\Gamma} = \boldsymbol{U}^*\boldsymbol{U}$ where $\boldsymbol{U}$ is an upper triangular matrix which converts $\boldsymbol{A}$ to a unitary matrix via similarity transformation: $\boldsymbol{A}^*\boldsymbol{\Gamma}\boldsymbol{A} = \boldsymbol{\Gamma} \Rightarrow \boldsymbol{A}^*\boldsymbol{U}^*\boldsymbol{U}\boldsymbol{A} = \boldsymbol{U}^*\boldsymbol{U} \Rightarrow \tilde{\boldsymbol{A}}^*\tilde{\boldsymbol{A}} = \boldsymbol{I}$, where

$$\tilde{\boldsymbol{A}} = \boldsymbol{U}\boldsymbol{A}\boldsymbol{U}^{-1} \tag{61}$$

This shows the eigenvalues of every lossless scattering matrix lie on the unit circle. It readily follows from similarity to $\tilde{\boldsymbol{A}}$ that $\boldsymbol{A}$ admits N linearly independent eigenvectors.

Conversely, assume $|\lambda_i| = 1$ for each eigenvalue λ_i of $\boldsymbol{A}$, and that there exists a matrix $\boldsymbol{T}$ of linearly independent eigenvectors of $\boldsymbol{A}$. Then the matrix $\boldsymbol{T}$ diagonalizes $\boldsymbol{A}$ to give $\boldsymbol{T}^{-1}\boldsymbol{A}\boldsymbol{T} = \boldsymbol{D} \Rightarrow \boldsymbol{T}^*\boldsymbol{A}^*\boldsymbol{T}^{-1^*} = \boldsymbol{D}^*$, where $\boldsymbol{D} = \mathrm{diag}(\lambda_1, \ldots, \lambda_N)$. Multiplying, we obtain $\boldsymbol{T}^*\boldsymbol{A}^*\boldsymbol{T}^{-1^*}\boldsymbol{T}^{-1}\boldsymbol{A}\boldsymbol{T} = \boldsymbol{D}^*\boldsymbol{D} = \boldsymbol{I} \Rightarrow \boldsymbol{A}^*\boldsymbol{T}^{-1^*}\boldsymbol{T}^{-1}\boldsymbol{A} = \boldsymbol{T}^{-1^*}\boldsymbol{T}^{-1}$. Thus, the condition of lossless scattering (26) is satisfied for $\boldsymbol{\Gamma} = \boldsymbol{T}^{-1^*}\boldsymbol{T}^{-1}$ which is Hermitian and positive definite.

Theorem 3 can be extended to lossless junctions of lossy waveguides, as the reader can easily verify by applying the above proof to (27).

It is worth noting that most research in *feedback delay networks* for artificial reverberation has been concerned only with orthogonal feedback matrices [42, 33] rather than on the more general class of matrices satisfying the losslessness condition (26) [78, 106, 79]. This is an excessive restriction since many of the matrices naturally arising from models of lossless physical junctions are not orthogonal. As can be seen above, physical scattering matrices are orthogonal only if we restrict attention to propagation in equal-admittance media [$\boldsymbol{\Gamma}(z) = \boldsymbol{I}$], or to propagation of normalized waves.

8 Complexity Reduction: A Physical Approach

The scattering matrix of a physical junction of N waveguides (38) can be expressed in terms of the alpha parameters as

$$\boldsymbol{A} = \boldsymbol{1}\boldsymbol{\alpha}^T - \boldsymbol{I} \tag{62}$$

where $\boldsymbol{\alpha}^T = \left[\begin{array}{cccc} \alpha_1 & \alpha_2 & \ldots & \alpha_N \end{array}\right]$, and in the lossless case,

$$\alpha_i \stackrel{\triangle}{=} 2\Gamma_i \Big/ \sum_{j=1}^{N} \Gamma_j. \tag{63}$$

The vector of outgoing pressure waves can be expressed as

$$\boldsymbol{p}^- = \boldsymbol{A}\boldsymbol{p}^+ \stackrel{\triangle}{=} \boldsymbol{1}p_J - \boldsymbol{p}^+ \tag{64}$$

where $p_J = \boldsymbol{\alpha}^T\boldsymbol{p}^+$ can be interpreted as the "junction pressure." Thus, the matrix-vector multiplication can be seen to require only N multiplications and $2N-1$ additions.

Equation (64) can be rewritten as

$$\begin{aligned} p_J &= \sum_{i=1}^{N} \alpha_i p_i^+, \qquad \alpha_i \stackrel{\triangle}{=} \frac{2\Gamma_i}{\Gamma_1 + \cdots + \Gamma_N} \\ p_j^- &= p_J - p_j^+ \end{aligned} \tag{65}$$

This is the canonical form of the scattering relations for a physical N-way scattering junction parametrized in terms of the alpha parameters.

Whenever possible, it is advisable to set the branch impedances so that $\alpha_i = 1$ for some i, and therefore only $N-1$ multiplications are needed. This is achieved when the ith waveguide admittance equals the sum of all the other admittances. According to Fettweis' terminology for wave digital filters, the ith junction port is called a *reflection-free port*, and the ith branch is said to be *adapted* to the other $N-1$ branches. Physically, a wave traveling into the junction on a reflection-free port will be fully scattered into the other branches meeting at the junction, with no reflection back along branch i.

In time-varying applications, it is also convenient to maintain scaling such that $\sum_{j=1}^{N} \Gamma_j = 1$ so that no divisions or renormalizations are necessary in the alpha parameters. This is easily accomplished by setting the admittance of branch 1, say, to

$$\Gamma_1(n) = 1 - \sum_{i=2}^{N} \Gamma_i(n) \tag{66}$$

provided this remains nonnegative.

Since the alpha parameters sum to 2 in the lossless case, the first element, say, of the vector $\boldsymbol{\alpha}$ can be expressed as

$$\alpha_1 = 2 - \sum_{i=2}^{N} \alpha_i \tag{67}$$

Thus, the vector of outgoing pressure waves can be computed as

$$\begin{aligned} \boldsymbol{p}^- &= \mathbf{1}\boldsymbol{\alpha}^T \boldsymbol{p}^+ - \boldsymbol{p}^+ \\ &= \mathbf{1}\left(2p_1^+ - \sum_{i=2}^{N} \alpha_i p_1^+ + \sum_{i=2}^{N} \alpha_i p_i^+\right) - \boldsymbol{p}^+ \\ &= \mathbf{1}\left[2p_1^+ + \sum_{i=2}^{N} \alpha_i (p_i^+ - p_1^+)\right] - \boldsymbol{p}^+ \end{aligned} \tag{68}$$

which implies

$$\begin{aligned} p_j^- &= 2p_1^+ + \sum_{i=2}^{N} \alpha_i (p_i^+ - p_1^+) - p_j^+ \\ &= p_1^- - \underbrace{(p_j^+ - p_1^+)}_{\text{available}} \end{aligned} \tag{69}$$

In Fettweis' terminology, the port corresponding to the first waveguide is called the *dependent port*. Organizing the computations as in (68), a scattering junction can be performed with $N-1$

multiplications and $3N-2$ additions instead of N multiplies and $2N-1$ additions using (64). Saving and reusing differences as implied in (69) eliminates another addition to get the number of [multiplies,adds] down to $[N-1, 3(N-1)]$ (see Fig. 6 for $N=2$). If we add the assumption that one of the ports is reflection-free, we get additional savings and use only $N-2$ multiplications and $3N-5$ adds [28]. Exploiting the dependent port leads to a small savings in the number of multiplies at the expense of an increase in the constant of proportionality in the number of adds. Nevertheless, for the case $N=2$, the formulation (69) is advantageous, since it can be implemented with one multiply and three adds.

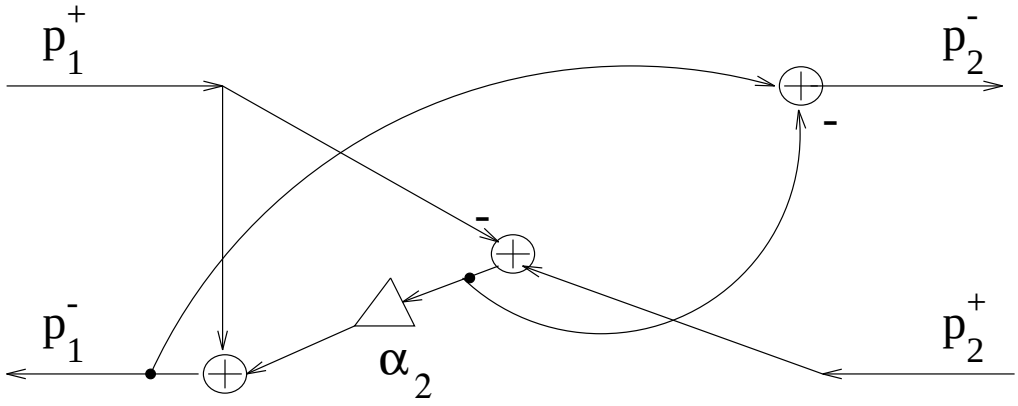

Figure 6: A one-multiply, three-add, scattering junction parametrized by an alpha parameter.

An important advantage provided by the organization of computations (68) and (69) is that they force the junction to be row allpass complementary (see section 5) even under coefficient quantization. The following theorem establishes the connection between allpass complementarity and structural losslessness of the scattering matrix.

Theorem 4 *Condition (67) (implying row allpass complementarity of the scattering matrix) is necessary and sufficient for structural losslessness of the physical scattering junction of N scalar waveguides in the presence of coefficient quantization.*

Proof: Denote the quantized scattering matrix by $\hat{\boldsymbol{A}} \stackrel{\triangle}{=} \mathbf{1}\hat{\boldsymbol{\alpha}}^T - \boldsymbol{I}$, where $\hat{\boldsymbol{\alpha}} = \boldsymbol{\alpha} - \boldsymbol{\epsilon}$, and $\boldsymbol{\epsilon} = [\epsilon_1, \ldots, \epsilon_N]^T$ is the vector of quantization errors in the alpha parameters $\alpha_i = \hat{\alpha}_i + \epsilon_i$. We must show that for every $\boldsymbol{\epsilon}$, there exists a positive-definite matrix $\hat{\boldsymbol{\Gamma}}$ such that $\hat{\boldsymbol{A}}^T\hat{\boldsymbol{\Gamma}}\hat{\boldsymbol{A}} = \hat{\boldsymbol{\Gamma}}$ exactly. Under the assumption that $\hat{\boldsymbol{\Gamma}}$ is diagonal, which follows from restriction to a physical junction of scalar waveguides, we need only find N positive diagonal elements $\hat{\Gamma}_i$ which satisfy the definition of losslessness of $\hat{\boldsymbol{A}}$. Let $\hat{\boldsymbol{\gamma}} = \hat{\boldsymbol{\Gamma}}\mathbf{1} = [\hat{\Gamma}_1, \ldots, \hat{\Gamma}_N]^T$ denote the vector of diagonal elements of $\hat{\boldsymbol{\Gamma}}$. Then losslessness requires

$$\begin{aligned}
\hat{\boldsymbol{\Gamma}} &= \hat{\boldsymbol{A}}^T\hat{\boldsymbol{\Gamma}}\hat{\boldsymbol{A}} \\
&= (\hat{\boldsymbol{\alpha}}\mathbf{1}^T - \boldsymbol{I})\hat{\boldsymbol{\Gamma}}(\mathbf{1}\hat{\boldsymbol{\alpha}}^T - \boldsymbol{I}) \\
&= \hat{\boldsymbol{\alpha}}\hat{\boldsymbol{\alpha}}^T(\mathbf{1}^T\hat{\boldsymbol{\gamma}}) - \hat{\boldsymbol{\alpha}}\hat{\boldsymbol{\gamma}}^T - \hat{\boldsymbol{\gamma}}\hat{\boldsymbol{\alpha}}^T + \hat{\boldsymbol{\Gamma}}
\end{aligned} \tag{70}$$

Thus, we must find positive $\hat{\Gamma}_i$ such that

$$\hat{\Gamma}_i\hat{\alpha}_j + \hat{\Gamma}_j\hat{\alpha}_i = \hat{\alpha}_i\hat{\alpha}_j\sum_{l=1}^{N}\hat{\Gamma}_l \tag{71}$$

Let $\hat{\Gamma}_i = c\hat{\alpha}_i/2$ where c is any positive constant. Since $\hat{\alpha}_i$ is positive, so is $\hat{\Gamma}_i$. (While $\hat{\alpha}_i$ is restricted to certain values, $\hat{\Gamma}_i$ may be any positive real value). The condition (71) becomes

$$\hat{\alpha}_i\hat{\alpha}_j c = \hat{\alpha}_i\hat{\alpha}_j c \sum_{l=1}^{N} \hat{\alpha}_l/2 \tag{72}$$

which holds if and only if

$$\sum_{l=1}^{N} \hat{\alpha}_l = 2 \tag{73}$$

and this identity is provided by condition (67).

We see that exact losslessness of a physical waveguide junction is assured provided only that the actual alpha parameters are positive and sum precisely to 2 *after* quantization. The proof extends readily to nonnegative $\hat{\alpha}_i$ by assigning $\hat{\Gamma}_i = 0$ to any waveguide branch corresponding to a port for which $\hat{\alpha}_i = 0$. (Note that $\hat{\alpha}_i = 0$ corresponds to a branch which contributes no signal to the junction, and a branch with zero admittance can convey no signal power. Such a situation is physically degenerate so that if quantization forces $\hat{\alpha}_i$ to zero for some i, the corresponding branch may be removed from the junction.)

The above theorem is quite simple from a physical point of view: All we require for exact losslessness is that the quantized scattering matrix correspond to *some* valid lossless scattering matrix. From the physical correspondence (63) between the alpha parameters and the branch wave admittances it is clear that losslessness holds when $\hat{\alpha}_1 + \cdots + \hat{\alpha}_N = 2$. For more general passivity, we can add a positive real "load" admittance Γ_L to the sum over Γ_j above to obtain that scattering passivity holds if and only if the alpha parameters are positive and sum to a value *not exceeding* 2.

The above discussion is only concerned with passivity of the scattering matrix itself. The application of the matrix is assumed to be exact. Since rounding of the final outgoing waves is necessary in practice, we add

Corollary 4 *Sufficient conditions for the passivity of a DWN are (1) all scattering matrices are passive, (2) intermediate outgoing waves are computed exactly at each junction in extended precision before rounding, and (3) the final outgoing waves from each junction are rounded passively.*

Since extended intermediate precision is required to ensure passivity, it is of interest to examine the additional bits required.

Theorem 5 *For an order N junction with m-bit alpha parameters ($m > 1$) and n-bit scalar wave variables ($n > 2$) computed in fixed point, the extended precision needed to implement the canonical scattering formula (64) is (a) one additional bit for the computation of junction pressure p_J, and (b) two additional bits for the computation of each outgoing wave p_j^-.*

Proof: From (64), assuming $0 < \alpha_i \leq 2$ and $-1 \leq p_i^+ < 1$, we have

$$|p_J| = \left|\sum_{i=1}^{N} \alpha_i p_i^+\right| \leq \sum_{i=1}^{N} \alpha_i \left|p_i^+\right| < \sum_{i=1}^{N} \alpha_i \leq 2$$

Hence (a) one additional bit is sufficient for the inner-product accumulator for p_J. That the extra bit is necessary is shown by taking $p_i^+ = -1$ for all i in which case $p_J = -2$ for any set of lossless alpha parameters.

The outgoing wave variables are computed as $p_i^- = p_J - p_i^+$, and a single bit is clearly sufficient to provide the needed headroom for a single subtraction in general. That the second headroom bit is necessary is shown by considering the example $N = 2$, $\alpha_1 = 0$, $\alpha_2 = 2$, $p_1^+ = 1/2$, $p_2^+ = -1$, in which case $p_1^- = -2 - 1/2 = -2.5$. If $\alpha_1 = 0$ is not allowed, then an example is obtained with $\alpha_1 = \epsilon_1$, $\alpha_2 = 2-\epsilon_1$, $p_1^+ = -1$, $p_2^+ = 1-\epsilon_2$, for which $p_1^- = (\epsilon_1-1)(-1)+(2-\epsilon_1)(1-\epsilon_2) = 3-2\epsilon_1-2\epsilon_2+\epsilon_1\epsilon_2$. For this to exceed 2, we must have $2\epsilon_1 + 2\epsilon_2 - \epsilon_1\epsilon_2 < 1$. With $m = 3$ or more, we can choose $\epsilon_1 = 1/4$, and with $n = 3$ or more, we can take $\epsilon_2 = 1/4$, and the inequality is satisfied. Thus, (b) two extra bits are necessary and sufficient for the computation of each outgoing wave variable p_j^-.

It is perhaps surprising at first that only one extra bit suffices for the junction pressure computation, no matter how many branches are impinging on the junction. Ordinarily, an inner product of length N requires $\log_2(N)$ headroom bits. The single headroom bit requirement is a direct result of the alpha parameters being restricted to positive partitions of 2 in the lossless case, or a positive partitioning of a positive number less than 2 in the lossy, passive case.

Since an out-of-range outgoing traveling wave typically must be "clipped" in practice (i.e., replaced by -1 if negative and $1 - \epsilon_2$ if positive), the two extra carry bits are normally fed along with the next lower bit (the in-range sign bit) to saturation logic which implements clipping as needed.

The computations (68) or (69) can also be used to implement precisely lossless or passive *time-varying* junctions. In this case, the passivity constraints become

$$\begin{aligned} \sum_{i=2}^{N} \alpha_i(n) &\le 2 \\ \alpha_i(n) &\ge 0 \end{aligned} \tag{74}$$

where n is time in samples, since α_1 implicitly obeys (67) in formulas (68) and (69). (Here we allow $\alpha_i(n) = 0$ which may be a convenient way to eliminate waveguide branches momentarily in the time-varying case.)

A junction of *normalized* waveguides can be obtained from (68) or (69) by transformer-coupling each branch other than the first with a waveguide having wave admittance Γ_1. The ideal transformer introduces two additional multiplications for each branch except one. Therefore, the normalized junction for arbitrary impedances can be implemented using $3(N-1)$ multiplications and $3(N-1)$ additions.

8.1 The Three-Multiply Normalized Lattice Section.

A well known two-port unnormalized scattering junction [57], implemented using one multiply and three adds, can be derived by organizing (64) as

$$\begin{aligned} p_1^- &= p_2^+ + p_\Delta \\ p_2^- &= p_1^+ + p_\Delta \end{aligned} \tag{75}$$

where

$$p_\Delta \stackrel{\triangle}{=} \rho(p_1^+ - p_2^+), \tag{76}$$

and

$$\rho \stackrel{\triangle}{=} \alpha_1 - 1 = 1 - \alpha_2 = \frac{\Gamma_1 - \Gamma_2}{\Gamma_1 + \Gamma_2} = \frac{R_2 - R_1}{R_2 + R_1} \tag{77}$$

is the *reflection coefficient* seen at an impedance step from R_1 to R_2, i.e., at port 1. In the ladder/lattice filter literature, only a 4-multiply, 2-add *normalized* junction appears to be known. A normalized, *three*-multiply junction can be obtained simply by coupling any one-multiply junction such as (75) with an ideal transformer [92] (see Appendix A), as illustrated in Fig. 7, where

$$g \triangleq \sqrt{\Gamma_2/\Gamma_1} \tag{78}$$

However, any lossless two-port junction which preserves a physical interpretation will do. For example, a transformer can also be attached to the alpha-parametrized one-multiply junction of Fig. 6 to obtain the three-multiply normalized junction of Fig. 8, having essentially the same properties as that of Fig. 7.

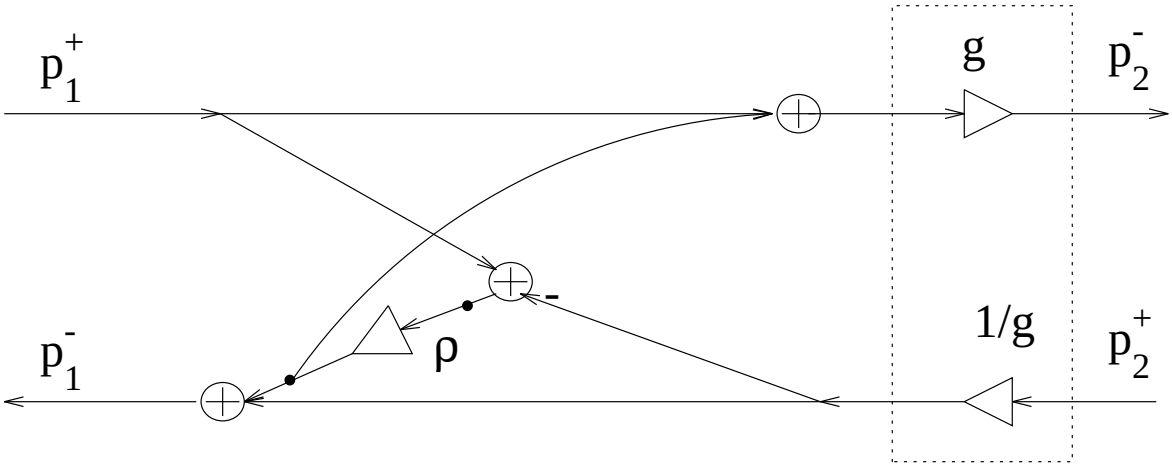

Figure 7: A three-multiply, three-add, normalized scattering junction parametrized in terms of a reflection coefficient.

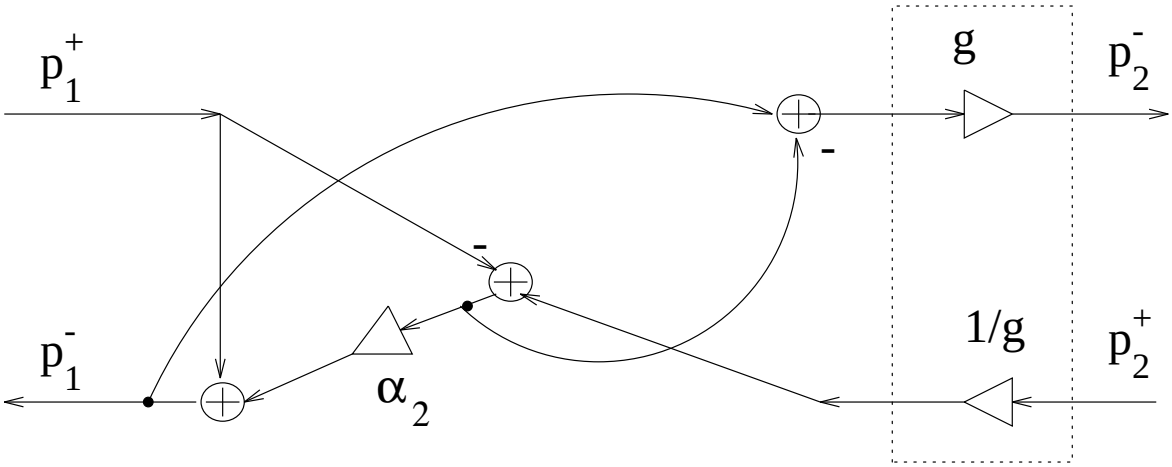

Figure 8: A three-multiply, three-add, normalized junction parametrized in terms of an alpha parameter.

Note that a high quality sinusoidal oscillator requiring only one multiply can be formed by

adding a unit delay on either side of a three-multiply junction and reflectively terminating (in which case the transformer multiplies cancel) [103].

One-multiply two-port scattering junctions enforce structural losslessness in finite precision arithmetic since the allpass complementarity condition (67) is always true. A *normalized* junction obtained by transformer-normalizing a one-multiply junction is also structurally lossless, provided the transformer multipliers are implemented in extended precision. In practice, normalized junctions of this type are made *passive* by using any non-amplifying rounding rule at the output. Denoting the ideal transformer coefficients by $g^- \stackrel{\triangle}{=} \sqrt{\Gamma_2/\Gamma_1}$ and $g^+ = 1/g^-$, the passivity condition on the transformer with quantized coefficients $\hat{g}^- = g^- - \epsilon^-$ and $\hat{g}^+ = g^+ - \epsilon^+$ is $\hat{g}^+\hat{g}^- \leq 1$, even in the time-varying case.

Since one of the transformer coefficients is always greater than 1, fixed-point implementations require support for an integer part, unlike the fractional fixed-point format used in most DSP chips. Since the transformer commutes with the junction in the two-port case, the larger coefficient can, without loss of generality, be chosen to apply to the signal entering the junction. As an example of the increased internal dynamic range required, if $\rho \in [-1+\epsilon, 1-\epsilon]$, the transformer coefficients may become as large as $\sqrt{2/\epsilon - 1}$. If ϵ is the "machine epsilon," i.e., $\epsilon = 2^{-(n-1)}$ for typical n-bit two's complement arithmetic normalized to lie in $[-1, 1)$, then the dynamic range of the transformer coefficients is bounded by $\sqrt{2^n - 1} \approx 2^{n/2}$. In summary, while transformer-normalized junctions trade a multiply for an add in the two-port case, they require up to 50% more bits of dynamic range within the junction adders.

9 Complexity Reduction: A Geometric Approach

A convenient expression for the scattering matrix of a junction of N normalized waveguides is obtained in terms of

$$\boldsymbol{u}_n^T \stackrel{\triangle}{=} \left[\begin{array}{cccc} \sqrt{\Gamma_1} & \sqrt{\Gamma_2} & \ldots & \sqrt{\Gamma_N} \end{array} \right] \tag{79}$$

The normalized scattering matrix $\tilde{\boldsymbol{A}}$ can then be expressed as

$$\tilde{\boldsymbol{A}} = 2\frac{\boldsymbol{u}\boldsymbol{u}^T}{\|\boldsymbol{u}\|^2} - \boldsymbol{I} \tag{80}$$

where $\|\boldsymbol{u}\|^2 \stackrel{\triangle}{=} \boldsymbol{u}^T\boldsymbol{u}$. Note that $\boldsymbol{u}$ is the eigenvector of $\tilde{\boldsymbol{A}}$ corresponding to the eigenvalue 1. A matrix of the form $-\tilde{\boldsymbol{A}}$ is known as a *Householder reflection* [34], and it produces the mirror image of a given vector about the hyperplane orthogonal to the vector $\boldsymbol{u}$.

The Householder structure (80) can be exploited to speed up the matrix-vector multiplication. Define

$$w \stackrel{\triangle}{=} \beta \boldsymbol{u}_n^T \boldsymbol{p}^+ \tag{81}$$

where $\beta = 2 / \| \boldsymbol{u}_n \|^2$. The computation of the outgoing waves can be expressed as:

$$\boldsymbol{p}^- = \tilde{\boldsymbol{A}}\boldsymbol{p}^+ = \boldsymbol{u}_n w - \boldsymbol{p}^+ \tag{82}$$

Thus, N multiplications and $N-1$ additions are needed to compute the scalar product in (81), and N multiplications and N additions are needed for the final multiply-add in (82). In the case of an acyclic network graph, we can eliminate at least one multiplication in (82) by scaling all impedances appropriately. A total of $2N-1$ multiplications and $2N-1$ additions are needed.

The unnormalized Householder reflection $\boldsymbol{H} = \| \boldsymbol{u}_n \|^2 \boldsymbol{I} - 2\boldsymbol{u}_n \boldsymbol{u}_n^T$ is structurally a unitary transformation in the sense that $\boldsymbol{H}^* \boldsymbol{H}$ remains a constant diagonal matrix after quantization of the vector $\boldsymbol{u}_n$ [110]. Hence, if all the incoming waves $\boldsymbol{p}^+$ are scaled by $\| \boldsymbol{u}_n \|^{-2}$, normalized junctions implemented in this way conserve their losslessness even under coefficient quantization. To be conservative, it is sufficient to scale the incoming waves by a constant slightly less than $\| \boldsymbol{u}_n \|^{-2}$, in such a way that the junction has a small loss. Preferably, however, we may scale the Γ_i so that they sum to 2^K for some integer K, in which case $\| \boldsymbol{u}_n \|^{-2}$ becomes a power of 2 implementable as a simple shift in fixed-point binary arithmetic.

Similarly, the unnormalized junction (38) can be interpreted as an "oblique Householder" reflection, in the sense that the sum of the vectors $\boldsymbol{p}^+$ and $\boldsymbol{p}^-$ is colinear with the vector $\left[\begin{array}{ccc} 1 & \ldots & 1 \end{array} \right]$ which lies on the diagonal of the parallelogram whose edges are given by the incoming and outgoing wave vectors. As we have already noticed in section 8, even in this case the matrix $\boldsymbol{A} = 2\boldsymbol{1}\boldsymbol{\Gamma}^T / < \boldsymbol{1}, \boldsymbol{\Gamma} > - \boldsymbol{I}$ can be implemented as a structurally lossless transformation, and therefore it is well suited as a building block for large networks using fixed-point computations.

Computations (64) and (82) do not lend themselves to highly parallel implementations because of the scalar product needed to compute w or p_J. A scalar product needs $O(\log_2 N)$ additions to be computed on $O(N)$ processors [55].

Yet Another Three-Multiply Normalized Lattice.

Further variations arise from analyzing the two-variable scattering junction algebraically. In the case of two arbitrary real, positive, scalar, waveguide impedances, the scattering relations are

$$\begin{aligned} \left[\begin{array}{c} p_1^- \\ p_2^- \end{array} \right] &= \left[\begin{array}{cc} \frac{2\Gamma_1}{\Gamma_1+\Gamma_2} - 1 & \frac{2\Gamma_2}{\Gamma_1+\Gamma_2} \\ \frac{2\Gamma_1}{\Gamma_1+\Gamma_2} & \frac{2\Gamma_2}{\Gamma_1+\Gamma_2} - 1 \end{array} \right] \left[\begin{array}{c} p_1^+ \\ p_2^+ \end{array} \right] \\ &= \boldsymbol{A} \left[\begin{array}{c} p_1^+ \\ p_2^+ \end{array} \right] \end{aligned} \tag{83}$$

The two-port normalized scattering matrix can be expressed as

$$\tilde{\boldsymbol{A}} = \left[\begin{array}{cc} \cos(\theta) & \sin(\theta) \\ \sin(\theta) & -\cos(\theta) \end{array} \right] \tag{84}$$

where

$$\cos(\theta) \stackrel{\triangle}{=} \frac{\Gamma_1 - \Gamma_2}{\Gamma_1 + \Gamma_2}, \qquad \sin(\theta) \stackrel{\triangle}{=} \frac{2\sqrt{\Gamma_1 \Gamma_2}}{\Gamma_1 + \Gamma_2}.$$

The matrix $\tilde{\boldsymbol{A}}$ is a (negated) Householder reflection, and it reflects any input across the line defined by the eigenvector $[\cos(\theta/2), \sin(\theta/2)]$. The quantities involved in (82) can be set to be $\boldsymbol{u}_n^T = \left[\begin{array}{cc} 1 & g \end{array} \right] = \left[\begin{array}{cc} 1 & \sqrt{\Gamma_2/\Gamma_1} \end{array} \right]$ and $\beta = \alpha_1 = 2\Gamma_1/(\Gamma_1 + \Gamma_2)$. The signal-flow graph obtained from (84) is the well-known normalized ladder section. The application of (82) in the two-port case leads to the signal-flow graph of Fig. 9.

It is worth noting that the realization of Fig. 9 can be implemented, for $\Gamma_1 > \Gamma_2$, with all coefficients in $[-2, 2)$, thereby needing only a one-bit integer part. Parametrizing in terms of the reflection coefficient $\rho = \alpha - 1$ can be used to confine all parameters to the range $[-1, 1)$, requiring no integer part. Note also that the junction computation consists of three sequential multiply-adds, as naturally fits the architecture of many current DSP chips.

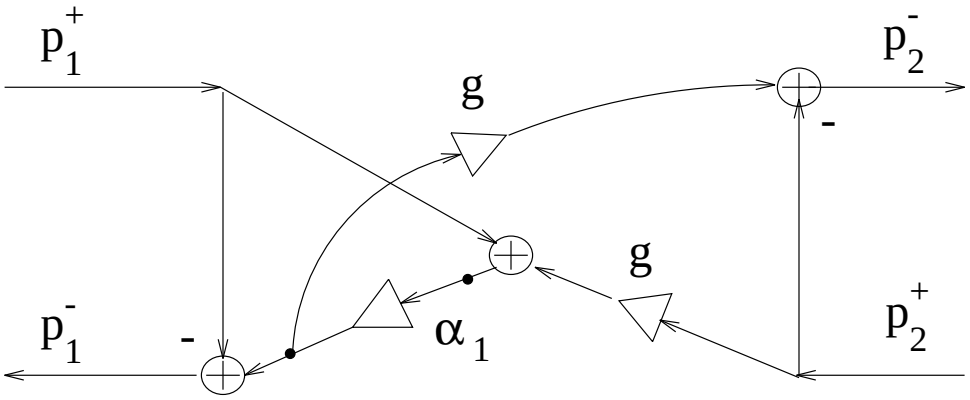

Figure 9: A three-multiply-add normalized junction.

The normalized 2-port junction can also be obtained by applying transformer coupling to a 2-multiply, 3-add unnormalized junction.

Consider the unnormalized 2×2 section in Kelly-Lochbaum form. Defining $\rho = \frac{\Gamma_1 - \Gamma_2}{\Gamma_1 + \Gamma_2}$, we can write the outgoing pressure wave on the left port as

$$\begin{aligned} p_1^- &= \rho p_1^+ + (1-\rho) p_2^+ \\ &= \rho p_1^+ + p_1^+ - p_1^+ + \frac{1-\rho}{1+\rho}(1+\rho) p_2^+ \\ &= \beta p_1^+ - p_1^+ + \frac{\Gamma_2}{\Gamma_1} \beta p_2^+ \\ &= -p_1^+ + \beta (p_1^+ + \frac{\Gamma_2}{\Gamma_1} p_2^+) \end{aligned} \tag{85}$$

For the right outgoing pressure wave we have

$$\begin{aligned} p_2^- &= (1+\rho) p_1^+ - \rho p_2^+ \\ &= \beta p_1^+ - \rho p_2^+ - p_2^+ + p_2^+ \\ &= \beta p_1^+ - p_2^+ + \frac{\Gamma_2}{\Gamma_1} \beta p_2^+ \\ &= -p_2^+ + \beta \left(p_1^+ + \frac{\Gamma_2}{\Gamma_1} p_2^+ \right) \end{aligned} \tag{86}$$

With these algebraic manipulations we have obtained the 2-multiply 3-add unnormalized junction. It does not offer any benefit over the classic lattice or ladder sections; however, now consider normalization via transformer coupling. Figure 10 shows how to obtain the 3-multiply-add junction of Fig. 9: after transformer coupling the 2-multiply junction, just push the transformer into the junction and consolidate the multipliers.

So far, we have obtained three alternative realizations of the three-multiply, three-add, normalized junction. By comparing Figures 7, 8 and 9, we can say that, for an implementation on a general purpose DSP chip with a parallel multiply-add instruction, the junction of Fig. 9 seems to offer some benefit over the other two. In fact, we can organize the computations into three multiply-adds in series, thus achieving a better pipeline. For VLSI design, the direct implementation of the matrix

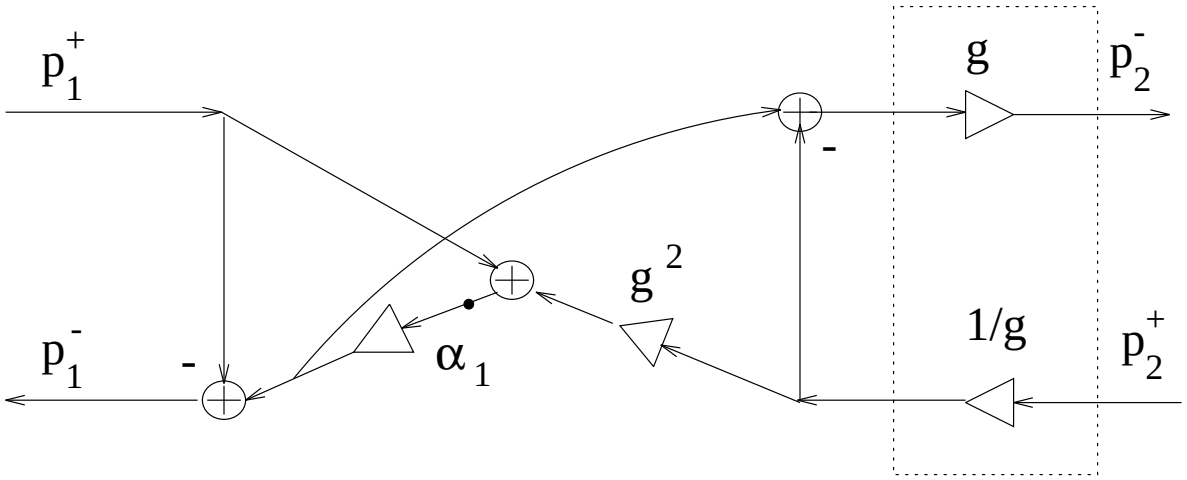

Figure 10: Obtaining a three-multiply-add normalized junction via transformer coupling.

product using the matrix (84) may be best, since it can be done with four parallel multiplications or CORDIC sections [38].

10 Non-constant scattering matrices and applications

The formulation of sections 3 and 4 can be restated for the more general case in which the scattering matrix has elements which are functions of z.

In this case the scattering relationship is

$$\boldsymbol{p}^-(z) = \boldsymbol{A}(z)\boldsymbol{p}^+(z) \tag{87}$$

In the case of lossless propagation, the scattering junction is said to be lossless if

$$\boldsymbol{\Gamma}(z) = \boldsymbol{A}^*(1/z^*)\boldsymbol{\Gamma}(z)\boldsymbol{A}(z) \tag{88}$$

In the more general case of passive propagation, the scattering junction is said to be lossless if

$$\boldsymbol{\Gamma}^*(1/z^*) = \boldsymbol{A}^*(1/z^*)\boldsymbol{\Gamma}(z)\boldsymbol{A}(z) \tag{89}$$

By adding (89) to its conjugate transpose we get

$$\boldsymbol{\Gamma}(z) + \boldsymbol{\Gamma}^*(1/z^*) = \boldsymbol{A}^*(1/z^*)[\boldsymbol{\Gamma}(z) + \boldsymbol{\Gamma}^*(1/z^*)]\boldsymbol{A}(z) \tag{90}$$

and we see that the construction of a normalized scattering matrix proceeds from a spectral factorization (if it exists) of the real part of the admittance matrix:

$$\boldsymbol{\Gamma}(z) + \boldsymbol{\Gamma}^*(1/z^*) = \boldsymbol{U}^*(1/z^*)\boldsymbol{U}(z) \tag{91}$$

When the medium is passive we have $\boldsymbol{\Gamma}(z) + \boldsymbol{\Gamma}^*(1/z^*) \geq \boldsymbol{0}$, and a spectral factorization does exist. The normalized scattering matrix is then

$$\tilde{\boldsymbol{A}}(z) = \boldsymbol{U}(z)\boldsymbol{A}(z)\boldsymbol{U}^{-1}(z) \tag{92}$$

and it is para-unitary, i.e.,

$$\tilde{\boldsymbol{A}}^*(1/z^*)\tilde{\boldsymbol{A}}(z) = \boldsymbol{I}\,. \tag{93}$$

A real-coefficient matrix $\tilde{\boldsymbol{A}}(z)$ which is analytic for $|z| \geq 1$ and which satisfies (93) is called *Lossless Bounded Real* [63, 112]. The condition (93) implies that the elements of any column of $\tilde{\boldsymbol{A}}(z)$ are power complementary, i.e.,

$$\sum_{i=1}^{N} |\, \tilde{a}_{i,k}(e^{j\omega})\, |^2 = 1\,. \tag{94}$$

In fixed-point implementations, the condition (94) can be satisfied as shown in [71, 83, 114]. Given a set of N power-complementary filters $\{\tilde{a}_{1,k}(z) \ldots \tilde{a}_{N,k}(z)\}$, they can be implemented by means of N allpass filters under mild conditions [114], and the property of power complementarity is structurally induced in the sense that coefficient quantization cannot alter it.

Applications of Generalized Scattering

The generalized scattering-matrix transfer function can be used to describe the intersection of conical acoustic tubes having different taper angles [96, 117, 130, 76]. Conical waveguides have a complex "one-pole" wave impedance in the continuous-time case [2, 5]. As a result, the elements of the scattering matrix for intersecting cones become first-order filters in place of real scattering coefficients. It turns out that the entire scattering junction for adjoined conical sections can be implemented using a single first-order IIR filter, analogous to the one-multiply lattice-filter junction [76], and "one-filter" forms exist also for the normalized case, in the presence of losses, and when there is a discontinuity in cross-sectional area (as in piecewise cylindrical acoustic tubes). In the discrete-time case, higher order filters and a guard band are necessary for high accuracy at all audio frequencies.

An interesting property of conical waveguide junctions is that the reflection coefficient corresponding to reflection from a *decreasing* taper angle (e.g., from a cylinder to a converging cone), is *unstable*. That is, the impulse response of such a junction contains a growing exponential component. The growing exponentials are always canceled by reflections (e.g., from the conical tip), but special care must be taken when using unstable one-pole filters in a practical model [131], or else FIR filters may be used to implement the truncated growing exponential impulse response including the canceling reflection from the other end of the converging conical segment [85]. Another promising approach (so far not implemented to our knowledge), is to choose normalized waves instead of pressure waves for the simulation.

Results similar to the conical junction are obtained for models of *toneholes* in woodwind bores [119, 115, 85]. In this application, the tonehole can be regarded as a three-port junction in which two of the ports connect to the bore on either side of the tonehole, and the third port connects to the tonehole itself. While the wave impedance of the bore is real for a cylindrical tube such as the clarinet, the tonehole presents a complex lumped impedance at the junction. (Alternatively, the tonehole can be modeled as an extremely short waveguide terminated by a simple reflection when closed and a complex radiation reflectance when open.) As in the case of intersecting cones, the reflection and transmission coefficients at the tonehole junction become one-pole filters in the continuous-time case, and third-order filters perform very well in the discrete-time case [85, 87]. In addition, it is possible to obtain low-order one-filter forms which handle all filtering in the tonehole junction [107]. However, unlike the conical junction case, the junction filter is always stable.

A third application similar to piecewise conical tube modeling and tonehole modeling is the modeling of *coupled strings* intersecting at a point driving a *lumped impedance* (e.g., a "bridge" model for a piano). Again, a "one-filter junction" is available [98], analogous to the one-multiply lattice-filter section. However, in this case, the one filter, while shared by all the strings, must contain all important body resonances (e.g., of a piano soundboard) "seen" through the bridge by the strings. A bridge filter is therefore not naturally a low-order filter. However, low-order approximations have been found to sound quite good, and it can be argued that strong coupling at isolated frequencies is musically undesirable. In other words, a smoother bridge reflectance, having a frequency response which follows only the upper envelope of the measured magnitude response, may be preferable.

The generalized scattering-matrix transfer function can also be used to simulate wave scattering by an object among discrete directions of arrival. If we consider N waveguides to simulate wave propagation along a set of N directions, the element $a_{i,j}$ of the scattering matrix can be interpreted as the coefficient applied to the signal coming in from direction j and being transmitted out along direction i. The scattering coefficients are highly dependent on frequency, and this can be handled using frequency-dependent elements of the scattering matrix. For example, wavelengths which are small compared with the object tend to reflect, or scatter according to the texture of the object surface, while wavelengths which are larger than the object tend to diffract around it and send scattering components in all directions. Consider the simpler case of incident wave energy scattering from a textured wall. In this case, wavelengths larger than the "grain size" of the texture tend to reflect specularly, while smaller wavelengths are scattered into a range of new directions according to well known formulas [52]. As a rough approximation for this case, we might use a single high-pass filter for all of the $N-1$ transmitted waves, and the complementary low-pass filter for the reflected wave, as in the "cross-over" scheme proposed by Regalia et al. [71]. In such a scheme, low frequencies are reflected specularly while high frequencies are diffusely reflected along $N-1$ directions.

11 Conclusions

A variety of topics related to digital waveguide networks (DWN) were discussed, within a generalized formulation which arises naturally from sampled traveling-wave solutions to physical wave equations. The idealized elements of DWNs are sampled lossless waveguides, or ideal transmission lines, intersecting at lossless scattering junctions. Such networks are a generalization of well known lattice and ladder digital filter structures, and many desirable properties of such filters are carried over. In physical modeling applications, lossy and dispersive waveguides and junctions are utilized, as are nonlinear and time-varying extensions.

Lossless junctions of normalized and unnormalized waveguides were investigated, and losslessness was characterized for both physical and non-physical junctions, in both energy-based and algebraic approaches. Depending on the application at hand, the energy-based viewpoint may be more advantageous over the algebraic viewpoint, or vice versa. For example, we introduced three new three-multiply, normalized, lattice-filter sections, each derived by adopting a different approach.

The main applications of digital waveguide networks so far seem to be in the fields of artificial reverberation, musical sound synthesis, and physical simulation of nearly lossless propagation in media such as air, plates, membranes, and vibrating strings. We expect future applications to be

plausible in any field needing numerically robust and computationally efficient simulation of largely linear propagation media, especially when the wave propagation is close to lossless, and when a fixed upper frequency limit makes sense in the application, as it does in most audio applications. In other terms, DWNs provide an effective "bandlimited medium" simulation, being especially efficient in the lossless case. Also, in many audio applications, it has proved sufficient to implement losses only sparsely in the DWN, using a single digital filter, e.g., to "summarize" the losses and dispersion over a fairly large section of medium, so that most of the efficiency of the lossless case is retained in the lossy, dispersive case. The time-varying case can be made free of "parametric amplification" effects by means of waveguide normalization. Finally, the nonlinear case, while not being bandlimited and therefore prone to aliasing, is greatly facilitated and made more robust by the use of a simulation structure which is precisely understood from a physical point of view.

Appendix A: The Digital Waveguide Transformer

A useful technique for junction normalization is by insertion of ideal transformers. First we define the ideal transformer in the 2×2 case (N=2) and apply it to the normalization of junctions where the impedance matrix is diagonal. Then we show a generalization to the $N \times N$ case and a non-diagonal impedance matrix.

The ideal cascade transformer is a lossless 2-port which scales up pressure by some factor and scales down velocity by the same factor without generating scattering reflections. Signal power is conserved. Since a transformer introduces a discontinuity in both pressure and velocity, it is not physical (although there are physical approximations used in microwave engineering). A conical acoustic tube section can be regarded as an approximate transformer, as can horn loudspeakers.

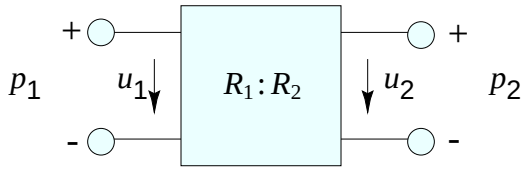

Consider the general two-port diagram in Fig. 11. Since a 2-port transformer, by definition, preserves signal power, we have

$$\begin{aligned} p_1 u_1 &= (p_1^+ + p_1^-)(p_1^+ - p_1^-)/R_1 \\ &= -(p_2^+ + p_2^-)(p_2^+ - p_2^-)/R_2 \\ &= -p_2 u_2 \end{aligned} \tag{95}$$

which is satisfied by

$$\begin{aligned} p_1^- &= \sqrt{\tfrac{R_1}{R_2}} p_2^+ \triangleq \tfrac{1}{g} p_2^+ \\ p_2^- &= \sqrt{\tfrac{R_2}{R_1}} p_1^+ \triangleq g p_1^+ \end{aligned} \tag{96}$$

where g is defined as the "turns ratio" since it corresponds to the voltage stepping ratio in electric transformers. Regarding the 2-port transformer as a special kind of two-waveguide junction, its

scattering matrix is

$$\Sigma = \left[\begin{array}{cc} 0 & \sqrt{\frac{R_1}{R_2}} \\ \sqrt{\frac{R_2}{R_1}} & 0 \end{array}\right] \triangleq \left[\begin{array}{cc} 0 & \frac{1}{g} \\ g & 0 \end{array}\right] \tag{97}$$

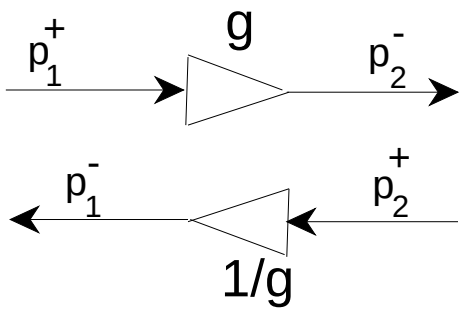

Figure 11: The ideal 2-port transformer.

The ideal 2-port transformer is depicted in Fig. 11.

In the case of a junction of N waveguides, we can normalize the junction by making all the waveguide impedances equal. This is accomplished by inserting N 2-port transformers, each of them coupling the original branch impedance at the junction with a unit impedance at each waveguide. This corresponds to the diagonal similarity transformation of (32). Of course, we can choose one of the original branch impedances as reference impedance, so that inserting $(N-1)$ 2-port transformers will suffice.

The physical interpretation of ideal transformers can be extended more generally. We define the generalized ideal transformer as a $2N$-port satisfying the equations [63]

$$\begin{array}{rcl} \boldsymbol{p}_1 & = & \boldsymbol{T}^* \boldsymbol{p}_2 \\ \boldsymbol{u}_2 & = & -\boldsymbol{T}\ \boldsymbol{u}_1 \end{array} \tag{98}$$

where $\boldsymbol{p}_1$ and $\boldsymbol{u}_1$ are respectively the N-component vectors of pressure and velocity at the first group of N ports, and $\mathbf{p}_2$ and $\boldsymbol{u}_2$ are the corresponding vectors for the second group of N ports. $\boldsymbol{T}$ is an $N \times N$ matrix called the *turns-ratio matrix*.

It is easy to check that the definition (98) satisfies the conservation of power:

$$\boldsymbol{u}_1{}^* \boldsymbol{p}_1 = -\boldsymbol{u}_2{}^* \boldsymbol{T}^{-1^*} \boldsymbol{T}^* \boldsymbol{p}_2 = -\boldsymbol{u}_2{}^* \boldsymbol{p}_2 \tag{99}$$

To normalize a junction in the general case of non-diagonal impedance matrix, we can use a transformer having turns-ratio matrix

$$\boldsymbol{T} = \boldsymbol{U}^{-1^*} \tag{100}$$

where $\boldsymbol{U}$ is the Cholesky factor of (33). The resulting scattering matrix is therefore given by (35).

We can say that the matrix $\boldsymbol{U}$ of (33) acts as an ideal transformer on the vector of all N waveguide variables.

An important application of the ideal transformer is to decouple scattering junctions from their attached waveguide branches. That is, by modulating the transformer "turns ratios," we may

arbitrarily modulate the scattering parameters without also modulating the signal power stored in the waveguide branches.

References

[1] *Handbook of Mathematical Functions*, New York: Dover, 1965.

[2] R. D. Ayers, L. J. Eliason, and D. Mahgerefteh, "The conical bore in musical acoustics," *American Journal of Physics*, vol. 53, pp. 528–537, June 1985.

[3] V. Belevitch, "Summary of the history of circuit theory," *Proceedings of the IRE*, vol. 50, pp. 848–855, May 1962.

[4] V. Belevitch, *Classical Network Theory*, San Francisco: Holden-Day, 1968.

[5] A. Benade, "Equivalent Circuits for Conical Waveguides," *Journal of the Acoustical Society of America*, vol. 83, pp. 1764–1769, May 1988.

[6] G. Borin and G. De Poli, "A Hammer-String Interaction Model for Physical Model Synthesis," in *Proc. XI Colloquium Mus. Inform.*, (Bologna, Italy), pp. 89–92, AIMI, Nov. 1995.

[7] G. Borin and G. De Poli, "A Hysteretic Hammer-String Interaction Model for Physical Model Synthesis," in *Proceedings of the Nordic Acoustical Meeting (NAM-96),* Helsinki, Finland, (Helsinki, Finland), pp. 399–406, June 1996.

[8] G. Borin, G. De Poli, and A. Sarti, *Sound Synthesis by Dynamic Systems Interaction*, vol. Readings in Computer-Generated Music, pp. 139–160, IEEE Computer Society Press, 1992, D. Baggi, editor.

[9] A. Bruckstein and T. Kailath, "An inverse scattering framework for several problems in signal processing," *IEEE Signal Processing Magazine*, vol. 4, pp. 6–20, January 1987.

[10] A. Chaigne, "On the Use of Finite Differences for Musical Synthesis. Application to Plucked Stringed Instruments," *J. Acoustique*, vol. 5, pp. 181–211, 1992.

[11] A. Chaigne and A. Askenfelt, "Numerical Simulations of Piano Strings. I. A Physical Model for a Struck String using Finite Difference Methods," *Journal of the Acoustical Society of America*, vol. 95, pp. 1112–1118, Feb 1994.

[12] J. Chung and K. K. Parhi, "Scaled normalized lattice digital filter structures," *IEEE Transactions on Circuits and Systems-II*, vol. 42, pp. 278–282, Apr. 1995.

[13] P. Cook, "Integration of physical modeling for synthesis and animation," in *Proceedings of the 1995 International Computer Music Conference, Banff*, pp. 525–528, Computer Music Association, 1995.

[14] P. R. Cook, *Identification of Control Parameters in an Articulatory Vocal Tract Model, with Applications to the Synthesis of Singing*, PhD thesis, Elec. Engineering Dept., Stanford University, Dec. 1990.

[15] P. R. Cook, "Tbone: An interactive waveguide brass instrument synthesis workbench for the NeXT machine," in *Proceedings of the 1991 International Computer Music Conference, Montreal*, pp. 297–299, Computer Music Association, 1991.

[16] P. R. Cook, "A meta-wind-instrument physical model, and a meta-controller for real time performance control," in *Proceedings of the 1992 International Computer Music Conference, San Jose*, pp. 273–276, Computer Music Association, 1992.

[17] P. R. Cook, "Singing voice synthesis: History, current work, and future directions," *Computer Music Journal*, vol. 20, pp. 38–46, Fall 1996.

[18] P. R. Cook, "Synthesis toolkit in C++, version 1.0," in *SIGGRAPH Proceedings*, Assoc. Comp. Mach., May 1996.

[19] L. Cremer, *The Physics of the Violin*, Cambridge, MA: MIT Press, 1984.

[20] J. l. d'Alembert, "Investigation of the curve formed by a vibrating string, 1747," in *Acoustics: Historical and Philosophical Development* (R. B. Linsdsay, ed.), pp. 119–123, Stroudsburg: Dowden, Hutchinson & Ross, 1973.

[21] G. De Poli and A. Sarti, "Generalized adaptors with memory for nonlinear wave digital structures," in *EUSIPCO*, (Trieste, Italy), pp. 1941–1944, Sept. 1996.

[22] J. R. Deller Jr., J. G. Proakis, and J. H. Hansen, *Discrete-Time Processing of Speech Signals*, New York: Macmillan, 1993.

[23] P. H. Dietz and N. Amir, "Synthesis of trumpet tones by physical modeling," in *Proceedings of the International Symposium on Musical Acoustics (ISMA-95), Dourdan, France*, (France), pp. 471–477, Société Français d'Acoustique, July 1995.

[24] W. C. Elmore and M. A. Heald, *Physics of Waves*, New York: McGraw Hill, 1969, Dover Publ., New York, 1985.

[25] K. T. Erickson and A. N. Michel, "Stability analysis of fixed-point digital filters using computer generated Lyapunov functions—Part I: Direct form and coupled form filters, and Part II: Wave digital filters and lattice digital filters," *IEEE Transactions on Circuits and Systems*, vol. 32, pp. 113–132 and 132–142, Feb. 1985.

[26] A. Fettweis, "Some Principles of Designing Digital Filters Imitating Classical Filter Structures," *IEEE Transactions on Circuit Theory*, vol. 18, pp. 314–316, Mar. 1971.

[27] A. Fettweis, "Wave Digital Filters: Theory and Practice," *Proceedings of the IEEE*, vol. 74, pp. 270–327, Feb. 1986.

[28] A. Fettweis and K. Meerkötter, "On Adaptors for Wave Digital Filters," *IEEE Transactions on Acoustics, Speech, Signal Processing*, vol. 23, pp. 516–524, Dec. 1975.

[29] J. L. Flanagan, K. Ishizaka, and K. L. Shipley, "Signal models for low bit-rate coding of speech," *Journal of the Acoustical Society of America*, vol. 68, no. 3, pp. 780–791, 1980.

[30] F. Fontana and D. Rocchesso, "Physical modeling of membranes for percussion instruments," *Acta Acustica*, vol. 84, pp. 529–542, May/June 1998.

[31] F. Fontana and D. Rocchesso, "Simulations of Membrane-based Percussion Instruments," in *Proc. Workshop: Sound Synthesis by Physical Modeling*, (Firenze, Italy), Centro Tempo Reale, June 1996.

[32] W. Frank and A. Lacroix, "Improved vocal tract models for speech synthesis," *Proceedings of the International Conference on Acoustics, Speech, and Signal Processing*, vol. 3, pp. 2011–2014, April 7–11 1986.

[33] M. A. Gerzon, "Unitary (Energy Preserving) Multichannel Networks with Feedback," *Electronics Letters V*, vol. 12, no. 11, pp. 278–279, 1976.

[34] G. H. Golub and C. F. V. Loan, *Matrix Computations*, Baltimore: The Johns Hopkins University Press, 1989.

[35] A. H. Gray and J. D. Markel, "A Normalized Digital Filter Structure," *IEEE Transactions on Acoustics, Speech, Signal Processing*, vol. 23, pp. 268–277, June 1975.

[36] S. Hirschman, *Digital Waveguide Modelling and Simulation of Reed Woodwind Instruments*, Engineer's thesis, Elec. Engineering Dept., Stanford University (CCRMA), May 1991, available as CCRMA Technical Report Stan-M-72, Music Dept., Stanford University, July 1991.

[37] S. Hirschman, P. R. Cook, and J. O. Smith, "Digital waveguide modelling of reed woodwinds: An interactive development environment on the NeXT computer," in *Proceedings of the 1991 International Computer Music Conference, Montreal*, pp. 300–303, Computer Music Association, 1991, available in "CCRMA Papers on Physical Modeling from the 1991 International Computer Music Conference," Department of Music Technical Report STAN-M-73, Stanford University, October 1991.

[38] Y. H. Hu, "CORDIC-Based VLSI Architectures for Digital Signal Processing," *IEEE Signal Processing Magazine*, pp. 16–35, July 1992.

[39] J. J. L. Kelly and C. C. Lochbaum, "Speech synthesis," *Proceedings of the Fourth International Congress on Acoustics, Copenhagen*, pp. 1–4, September 1962, Paper G42.

[40] D. A. Jaffe and J. O. Smith, "Extensions of the Karplus-Strong Plucked String Algorithm," *Computer Music Journal*, vol. 7, no. 2, pp. 56–69, 1983.

[41] D. A. Jaffe and J. O. Smith, "Performance expression in commuted waveguide synthesis of bowed strings," in *Proceedings of the 1995 International Computer Music Conference, Banff*, pp. 343–346, Computer Music Association, 1995.

[42] J.-M. Jot and A. Chaigne, "Digital Delay Networks for Designing Artificial Reverberators," in *Audio Engineering Society Convention*, (Paris, France), AES, Feb. 1991.

[43] T. Kailath, *Linear Systems*, Englewood Cliffs: Prentice-Hall, 1980.

[44] M. Karjalainen and U. K. Laine, "A model for real-time sound synthesis of guitar on a floating-point signal processor," in *Proceedings of the International Conference on Acoustics, Speech, and Signal Processing, Toronto*, vol. 5, (New York), pp. 3653–3656, IEEE Press, May 1991.

[45] M. Karjalainen and J. O. Smith, "Body modeling techniques for string instrument synthesis," in *Proceedings of the 1996 International Computer Music Conference, Hong Kong*, pp. 232–239, Computer Music Association, Aug. 1996.

[46] M. Karjalainen, U. K. Laine, T. I. Laakso, and V. Välimäki, "Transmission-Line Modeling and Real-Time Synthesis of String and Wind Instruments," in *Proc. International Computer Music Conference*, (Montreal, Canada), pp. 293–296, ICMA, 1991.

[47] M. Karjalainen, J. Backman, and J. Pölkki, "Analysis, Modeling, and Real-Time Sound Synthesis of the Kantele, A Traditional Finnish String Instrument," in *Proceedings of the International Conference on Acoustics, Speech, and Signal Processing*, (Minneapolis), pp. 229–232, IEEE, 1993.

[48] M. Karjalainen, V. Välimäki, and Z. Jánosy, "Towards High-Quality Sound Synthesis of the Guitar and String Instruments," in *Proc. International Computer Music Conference*, (Tokyo, Japan), pp. 56–63, ICMA, 1993.

[49] M. Karjalainen, V. Välimäki, B. Hernoux, and J. Huopaniemi, "Exploration of wind instruments using digital signal processing and physical modeling techniques," in *Proceedings of the 1995 International Computer Music Conference, Banff*, pp. 509–516, Computer Music Association, 1995, Revised version published in the *Journal of New Music Research*, 24(4), December 1995.

[50] E. Keller, *Fundamentals of Speech Synthesis*, New York: John Wiley and Sons, Inc., 1994.

[51] S.-Y. Kung, "On supercomputing with systolic/wavefront array processors," *Proceedings of the IEEE*, vol. 72, pp. 867–884, July 1984.

[52] H. Kuttruff, *Room Acoustics*, Essex, England: Elsevier Science, 1991, Third Ed.; First Ed. 1973.

[53] T. I. Laakso, V. Välimäki, M. Karjalainen, and U. K. Laine, "Splitting the Unit Delay—Tools for Fractional Delay Filter Design," *IEEE Signal Processing Magazine*, vol. 13, pp. 30–60, January 1996.

[54] A. Lacroix and B. Makai, "A novel vocoder concept based on discrete time acoustic tubes," *Proceedings of the International Conference on Acoustics, Speech, and Signal Processing, Washington, D.C.*, pp. 73–76, April 2–4 1979.

[55] F. T. Leighton, *Introduction to Parallel Algorithms and Architectures : Arrays, Trees, Hypercubes*, Los Altos, California: William Kaufmann, Inc., 1992.

[56] I. T. Lim and B. G. Lee, "Lossless Pole-Zero Modeling of Speech Signals," *IEEE Transactions on Speech and Audio Processing*, vol. 1, pp. 269–276, July 1993.

[57] J. D. Markel and A. H. Gray, *Linear Prediction of Speech*, New York: Springer-Verlag, 1976.

[58] K. Meerkotter and R. Scholtz, "Digital simulation of nonlinear circuits by wave digital filter principles," in *IEEE Proc. ISCAS '89*, (New York), pp. 720–723, IEEE Press, 1989.

[59] R. K. Miller and A. N. Michel, *Ordinary Differential Equations*, New York: Academic Press, 1982.

[60] P. M. Morse, *Vibration and Sound*, New York: American Institute of Physics for the Acoustical Society of America, 1991, 1st ed. 1936, 2nd ed. 1948.

[61] P. M. Morse and K. U. Ingard, *Theoretical Acoustics*, New York: McGraw-Hill, 1968, Reprinted in 1986, Princeton Univ. Press, Princeton, NJ.

[62] P. J. Moylan, "Implications of passivity in a class of nonlinear systems," *IEEE Transactions on Automatic Control*, vol. 19, pp. 373–381, Aug. 1974.

[63] R. W. Newcomb, *Linear Multiport Synthesis*, New York: McGraw-Hill, 1966.

[64] A. Paladin and D. Rocchesso, "A Dispersive Resonator in Real Time on MARS Workstation," in *Proc. International Computer Music Conference* (A. Strange, ed.), (San Jose, CA), pp. 146–149, ICMA, Oct. 1992.

[65] T. W. Parks and C. S. Burrus, *Digital Filter Design*, New York: John Wiley and Sons, Inc., 1987.

[66] S. Perlis, *Theory of Matrices*, Reading, Mass.: Addison-Wesley, 1952.

[67] J. R. Pierce and S. A. Van Duyne, "A passive nonlinear digital filter design which facilitates physics-based sound synthesis of highly nonlinear musical instruments," *Journal of the Acoustical Society of America*, vol. 101, pp. 1120–1126, Feb. 1997.

[68] N. Porcaro, P. Scandalis, D. Jaffe, and J. O. Smith, "Using SynthBuilder for the creation of physical models," in *Proceedings of the 1996 International Computer Music Conference, Hong Kong*, Computer Music Association, 1996.

[69] G. Putland, "Every one-parameter acoustic field obeys webster's horn equation," *Journal of the Audio Engineering Society*, vol. 41, pp. 435–451, June 1993.

[70] W. Putnam and J. O. Smith, "Design of fractional delay filters using convex optimization," in *Proceedings of the IEEE Workshop on Applications of Signal Processing to Audio and Acoustics, New Paltz, NY*, (New York), IEEE Press, Oct. 1997, `http://ccrma.stanford.edu/~jos/resample/optfir.pdf`.

[71] P. A. Regalia, S. K. Mitra, and P. P. Vaidyanathan, "The Digital All-Pass Filter: A Versatile Signal Processing Building Block," *Proceedings of the IEEE*, vol. 76, pp. 19–37, Jan. 1988.

[72] J. D. Rhodes, P. C. Marston, and D. C. Youla, "Explicit solution for the synthesis of two-variable transmission-line networks," *IEEE Transactions on Circuit Theory*, vol. CT-20, pp. 504–511, Sept. 1973.

[73] C. Roads, *The Computer Music Tutorial*, Cambridge, MA: MIT Press, 1996.

[74] C. Roads, S. T. Pope, A. Piccialli, and G. De Poli, eds., *Musical Signal Processing*, Netherlands: Swets and Zietlinger, 1997.

[75] R. A. Roberts and C. T. Mullis, *Digital Signal Processing*, Reading - MA: Addison-Wesley, 1987.

[76] D. Rocchesso, *Strutture ed Algoritmi per l'Elaborazione del Suono basati su Reti di Linee di Ritardo Interconnesse*, Phd thesis, Università di Padova, Dipartimento di Elettronica e Informatica, Feb. 1996.

[77] D. Rocchesso and F. Scalcon, "Accurate Dispersion Simulation for Piano Strings," in *Proceedings of the Nordic Acoustical Meeting (NAM-96),* Helsinki, Finland, pp. 407–414, June 1996.

[78] D. Rocchesso and J. O. Smith, "Circulant Feedback Delay Networks for Sound Synthesis and Processing," in *Proc. International Computer Music Conference*, (Aarhus, Denmark), pp. 378–382, ICMA, Sept. 1994.

[79] D. Rocchesso and J. O. Smith, "Circulant and Elliptic Feedback Delay Networks for Artificial Reverberation," *IEEE Transactions on Speech and Audio Processing*, vol. 5, no. 1, pp. 51–63, 1996.

[80] D. Rocchesso and F. Turra, "A Generalized Excitation for Real-Time Sound Synthesis by Physical Models," in *Proc. of the Stockholm Music Acoustics Conf.* (A. Friberg, J. Iwarsson, E. Jansson, and J. Sundberg, eds.), (Stockholm), pp. 584–588, Royal Swedish Academy of Music, July 1993.

[81] X. Rodet, "Flexible yet controllable physical models: A nonlinear dynamics approach," in *Proceedings of the 1993 International Computer Music Conference, Tokyo*, pp. 10–15, Computer Music Association, 1993.

[82] X. Rodet, "One and two mass model oscillations for voice and instruments," in *Proceedings of the 1995 International Computer Music Conference, Banff*, pp. 207–214, Computer Music Association, 1995.

[83] T. Saramäki, "On the Design of Digital Filters as a Sum of Two All-Pass Filters," *IEEE Transactions on Circuits and Systems*, vol. 32, pp. 1191–1193, Nov. 1985.

[84] L. Savioja, J. Backman, A. Järvinen, and T. Takala, "Waveguide Mesh Method for Low-Frequency Simulation of Room Acoustics," *Proceedings of the 15th International Conference on Acoustics (ICA-95),* Trondheim, Norway, pp. 637–640, June 1995.

[85] G. Scavone, *An Acoustic Analysis of Single-Reed Woodwind Instruments with an Emphasis on Design and Performance Issues and Digital Waveguide Modeling Techniques*, PhD thesis, Music Department, March 1997, In preparation; date estimated.

[86] G. Scavone and J. O. Smith, "Digital waveguide modeling of woodwind toneholes," in *Proceedings of the 1997 International Computer Music Conference, Greece*, Computer Music Association, 1997.

[87] G. Scavone and J. O. Smith, "Scattering parameters for the Keefe clarinet tonehole model," in *Proceedings of the International Symposium on Musical Acoustics (ISMA-97), Edinburgh, Scotland*, pp. 433–438, Aug. 1997.

[88] R. W. Schafer and L. R. Rabiner, "A digital signal processing approach to interpolation," *Proceedings of the IEEE*, vol. 61, pp. 692–702, June 1973.

[89] J. Schroeter and M. M. Sondhi, "Techniques for estimating vocal-tract shapes from the speech signal," *IEEE Transactions on Speech and Audio Processing*, vol. 2, pp. 133–150, Jan. 1994.

[90] J. O. Smith, *Techniques for Digital Filter Design and System Identification with Application to the Violin*, PhD thesis, Elec. Engineering Dept., Stanford University, June 1983.

[91] J. O. Smith, "A New Approach to Digital Reverberation Using Closed Waveguide Networks," in *Proc. International Computer Music Conference*, (Vancouver, Canada), pp. 47–53, ICMA, 1985, Also available in [93].

[92] J. O. Smith, "Elimination of limit cycles and overflow oscillations in time-varying lattice and ladder digital filters," Tech. Rep. STAN–M–35, CCRMA, Music Department, Stanford University, May 1986, Short version published in *Proceedings of the IEEE Conference on Circuits and Systems, San Jose*, May 1986. Full version also available in [93].

[93] J. O. Smith, "Music applications of digital waveguides," Tech. Rep. STAN–M–39, CCRMA, Music Department, Stanford University, 1987, A compendium containing four related papers and presentation overheads on digital waveguide reverberation, synthesis, and filtering. CCRMA technical reports can be ordered by calling (415)723-4971 or by sending an email request to hmk@ccrma.stanford.edu.

[94] J. O. Smith, "Waveguide filter tutorial," in *Proceedings of the 1987 International Computer Music Conference, Champaign-Urbana*, pp. 9–16, Computer Music Association, 1987.

[95] J. O. Smith, "Waveguide digital filters," in *Music Applications of Digital Waveguides*, CCRMA, 1987, Part IV of [93].

[96] J. O. Smith, "Waveguide simulation of non-cylindrical acoustic tubes," in *Proceedings of the 1991 International Computer Music Conference, Montreal*, pp. 304–307, Computer Music Association, 1991.

[97] J. O. Smith, "Physical modeling using digital waveguides," *Computer Music Journal*, vol. 16, pp. 74–91, Winter 1992, special issue: Physical Modeling of Musical Instruments, Part I. `http://-ccrma.stanford.edu/~jos/pmudw/`.

[98] J. O. Smith, "Efficient synthesis of stringed musical instruments," in *Proceedings of the 1993 International Computer Music Conference, Tokyo*, pp. 64–71, Computer Music Association, 1993.

[99] J. O. Smith, "Use of commutativity in simplifying acoustic simulations," in *Proceedings of the IEEE Workshop on Applications of Signal Processing to Audio and Acoustics*, (New York), IEEE Press, Oct. 1993.

[100] J. O. Smith, "Physical modeling synthesis update," *Computer Music Journal*, vol. 20, pp. 44–56, Summer 1996.

[101] J. O. Smith, "Acoustic modeling using digital waveguides," in *Musical Signal Processing* (C. Roads, S. T. Pope, A. Piccialli, and G. De Poli, eds.), pp. 221–263, Netherlands: Swets and Zietlinger, 1997.

[102] J. O. Smith, "Principles of digital waveguide models of musical instruments," in *Applications of Digital Signal Processing to Audio and Acoustics* (M. Kahrs and K. Brandenburg, eds.), pp. 417–466, Boston/Dordrecht/London: Kluwer Academic Publishers, 1998.

[103] J. O. Smith and P. R. Cook, "The second-order digital waveguide oscillator," in *Proceedings of the 1992 International Computer Music Conference, San Jose*, pp. 150–153, Computer Music Association, San 1992, Available online at http://www-ccrma.stanford.edu/~jos/.

[104] J. O. Smith and B. Friedlander, "Adaptive Interpolated Time-Delay Estimation," *IEEE Transactions on Aerospace and Electronic Systems*, vol. 21, pp. 180–199, Mar. 1985.

[105] J. O. Smith and P. Gossett, "A flexible sampling-rate conversion method," in *Proceedings of the International Conference on Acoustics, Speech, and Signal Processing*, vol. 2, (San Diego), pp. 19.4.1–19.4.2, IEEE Press, March 1984, An expanded tutorial based on this paper and associated free software are available online under http://www-ccrma.stanford.edu/~jos.

[106] J. O. Smith and D. Rocchesso, "Connection between Feedback Delay Networks and Waveguide Networks for Digital Reverberation," in *Proc. International Computer Music Conference*, (Aarhus, Denmark), pp. 376–377, ICMA, Sept. 1994.

[107] J. O. Smith and G. Scavone, "The one-filter Keefe clarinet tonehole," in *Proceedings of the IEEE Workshop on Applications of Signal Processing to Audio and Acoustics, New Paltz, NY*, (New York), IEEE Press, Oct. 1997.

[108] T. Stilson, "Forward-going wave extraction in acoustic tubes," in *Proceedings of the 1995 International Computer Music Conference, Banff*, pp. 517–520, Computer Music Association, 1995.

[109] J. Strikwerda, *Finite Difference Schemes and Partial Differential Equations*, Pacific Grove, CA: Wadsworth and Brooks, 1989.

[110] P. P. Vaidyanathan, *Multirate Systems and Filter Banks*, Englewood Cliffs, NY: Prentice Hall, 1993.

[111] P. P. Vaidyanathan and S. K. Mitra, "Low Passband Sensitivity Digital Filters: A Generalized Viewpoint and Synthesis Procedures," *Proceedings of the IEEE*, vol. 72, pp. 404–423, Apr. 1984.

[112] P. P. Vaidyanathan and S. K. Mitra, "A General Family of Multivariable Digital Lattice Filters," *IEEE Transactions on Circuits and Systems*, vol. 32, pp. 1234–1245, Dec. 1985.

[113] P. P. Vaidyanathan and S. K. Mitra, "Passivity Properties of Low-Sensitivity Digital Filter Structures," *IEEE Transactions on Circuits and Systems*, vol. 32, pp. 217–223, Mar. 1985.

[114] P. P. Vaidyanathan, S. K. Mitra, and Y. Neuvo, "A New Approach to the Realization of Low-Sensitivity IIR Digital Filters," *IEEE Transactions on Acoustics, Speech, Signal Processing*, vol. 34, pp. 350–361, Apr. 1986.

[115] V. Välimäki, *Discrete-Time Modeling of Acoustic Tubes Using Fractional Delay Filters*, PhD thesis, Report no. 37, Helsinki University of Technology, Faculty of Elec. Eng., Lab. of Acoustic and Audio Signal Processing, Espoo, Finland, Dec. 1995.

[116] V. Välimäki and M. Karjalainen, "Digital Waveguide Modeling of Wind Instrument Bores Constructed of Truncated Cones," in *Proc. International Computer Music Conference*, (Aarhus, Denmark), pp. 423–430, ICMA, 1994.

[117] V. Välimäki and M. Karjalainen, "Improving the Kelly-Lochbaum vocal tract model using conical tube sections and fractional delay filtering techniques," in *Proc. 1994 International Conference on Spoken Language Processing (ICSLP-94)*, vol. 2, (Yokohama, Japan), pp. 615–618, IEEE Press, Sept. 18–22 1994.

[118] V. Välimäki and M. Karjalainen, "Implementation of Fractional Delay Waveguide Models using Allpass Filters," in *Proceedings of the International Conference on Acoustics, Speech, and Signal Processing*, (Detroit), pp. 8–12, IEEE, May 1995.

[119] V. Välimäki, M. Karjalainen, and T. I. Laakso, "Modeling of Woodwind Bores with Finger Holes," in *Proc. International Computer Music Conference*, (Tokyo, Japan), pp. 32–39, ICMA, 1993.

[120] V. Välimäki, T. I. Laakso, and J. Mackenzie, "Elimination of Transients in Time-Varying Allpass Fractional Delay Filters with Application to Digital Waveguide Modeling," in *Proc. International Computer Music Conference*, (Banff, Canada), pp. 327–334, ICMA, 1995.

[121] V. Välimäki, J. Huopaniemi, M. Karjalainen, and Z. Jánosy, "Physical Modeling of Plucked String Instruments with Application to Real-Time Sound Synthesis," *Audio Engineering Society Convention*, vol. Preprint 3956, Feb 1995, Submitted to the Journal of the Audio Engineering Society.

[122] S. A. Van Duyne and J. O. Smith, "Physical Modeling with the 2-D Digital Waveguide Mesh," in *Proc. International Computer Music Conference*, (Tokyo, Japan), pp. 40–47, ICMA, 1993.

[123] S. A. Van Duyne and J. O. Smith, "The 2-D Digital Waveguide Mesh," in *Proceedings of the IEEE Workshop on Applications of Signal Processing to Audio and Acoustics*, (Mohonk, NY), IEEE, 1993.

[124] S. A. Van Duyne and J. O. Smith, "The Tetrahedral Digital Waveguide Mesh," in *Proceedings of the IEEE Workshop on Applications of Signal Processing to Audio and Acoustics*, (Mohonk, NY), IEEE, Oct. 1995.

[125] S. A. Van Duyne and J. O. Smith, "The Tetrahedral Waveguide Mesh: Multiply-Free Computation of Wave Propagation in Free Space," in *Proceedings of the IEEE Workshop on Applications of Signal Processing to Audio and Acoustics*, (Mohonk, NY), Oct. 1995.

[126] S. A. Van Duyne, J. R. Pierce, and J. O. Smith, "Traveling Wave Implementation of a Lossless Mode-Coupling Filter and the Wave Digital Hammer," in *Proc. International Computer Music Conference*, (Aarhus, Denmark), pp. 411–418, ICMA, Sept. 1994.

[127] S. A. Van Duyne, J. R. Pierce, and J. O. Smith, "Traveling-wave implementation of a lossless mode-coupling filter and the wave digital hammer," in *Proceedings of the 1994 International Computer Music Conference, Århus*, pp. 411–418, Computer Music Association, 1994, Also presented at the conference of the Acoustical Society of America, Nov., 1994.

[128] M. E. Van Valkenburg, *Introduction to Modern Network Synthesis*, New York: John Wiley and Sons, Inc., 1960.

[129] M. E. Van Valkenburg, *Introduction to Modern Network Synthesis*, New York: John Wiley and Sons, Inc., 1960.

[130] M. van Walstijn and G. de Bruin, "Conical waveguide filters," in *Proceedings of the Second International Conference on Acoustics and Musical Research*, (Ferrara, Italy), pp. 47–54, CIARM, May 1995.

[131] A. Wang and J. O. Smith, "On fast fir filters implemented as tail-canceling iir filters," *IEEE Transactions on Signal Processing*, vol. 45, 1997, Accepted for publication.

[132] G. Weinreich, "Coupled Piano Strings," *Journal of the Acoustical Society of America*, vol. 62, pp. 1474–1484, Dec. 1977.

[133] M. R. Wohlers, *Lumped and Distributed Passive Networks*, New York: Academic Press, Inc., 1969.

[134] Yamaha Corp., "Yamaha VL-1 User's Manual," 1993.

Julius O. Smith received the B.S.E.E. degree from Rice University, Houston, TX, in 1975. He received the M.S. and Ph.D. degrees in E.E. from Stanford University, Stanford, CA, in 1978 and 1983, respectively. His Ph.D. research involved the application of digital signal processing and system identification techniques to the modeling and synthesis of the violin, clarinet, reverberant spaces, and other musical systems. From 1975 to 1977 he worked in the Signal Processing Department at ESL, Sunnyvale, CA, on systems for digital communications. From 1982 to 1986 he was with the Adaptive Systems Department at Systems Control Technology, Palo Alto, CA, where he worked in the areas of adaptive filtering and spectral estimation. From 1986 to 1991 he was employed at NeXT Computer, Inc., responsible for sound, music, and signal processing software for the NeXT computer workstation. Since then he has been an Associate Professor at the Center for Computer Research in Music and Acoustics (CCRMA) at Stanford teaching courses in signal processing and music technology, and pursuing research in signal processing techniques applied to music and audio. For more information, see http://ccrma.stanford.edu/~jos/.

Davide Rocchesso is a PhD candidate at the Dipartimento di Elettronica e Informatica, Università di Padova - Italy. He received his Electrical Engineering degree from the Università di Padova in 1992, with a dissertation on real-time physical modeling of music instruments. In 1994 and 1995, he was visiting scholar at the Center for Computer Research in Music and Acoustics (CCRMA), Stanford University. He has been collaborating with the Centro di Sonologia Computazionale (CSC) dell'Università di Padova since 1991, as a researcher and a live-electronic designer/performer. His main interests are in audio signal processing, physical modeling, sound reverberation and spatialization, parallel algorithms. Since 1995 he has been a member of the Board of Directors of the Associazione di Informatica Musicale Italiana (AIMI).